PULSE VOLUME SENSING AND ANALYSIS FOR ADVANCED BLOOD PRESSURE MONITORING

By

Keerthana Natarajan

A DISSERTATION

Submitted to
Michigan State University
in partial fulfillment of the requirements
for the degree of

Electrical Engineering – Doctor of Philosophy

2021

ABSTRACT

PULSE VOLUME SENSING AND ANALYSIS FOR
ADVANCED BLOOD PRESSURE MONITORING

By

Keerthana Natarajan

Approximately a quarter of the world's population is affected by high blood pressure (BP). It is a major risk factor for stroke and heart disease, which are leading causes of mortality. Management of hypertension could be improved by increased accuracy and convenience of BP measurement devices. Existing devices are not convenient or portable enough. In this work, we investigate three approaches to improve the accuracy and convenience of BP measurement.

A physiologic method was developed to further advance central BP measurement. A patient-specific method was applied to estimate brachial BP levels from a cuff pressure waveform obtained during conventional deflation via a nonlinear arterial compliance model. A physiologically-inspired method was then employed to extract the PVP waveform from the same waveform via ensemble averaging and calibrate it to the brachial BP levels. A method based on a wave reflection model was thereafter employed to define a variable transfer function, which was applied to the calibrated waveform to derive central BP. This method was evaluated against invasive central BP measurements from patients. The method yielded central systolic, diastolic, and pulse pressure bias and precision errors of −0.6 to 2.6 and 6.8 to 9.0 mmHg. The conventional oscillometric method produced similar bias errors but precision errors of 8.2 to 12.5 mmHg ($p \leq 0.01$). The new method can derive central BP more reliably than some current non-invasive devices and in the same way as traditional cuff BP.

We then developed an iPhone X application to measure cuff-less BP via the "oscillometric finger pressing method". The user presses her fingertip on both the front camera and screen to increase the external pressure of the underlying artery, while the application measures the resulting variable-amplitude blood volume oscillations via the camera and applied pressure via the strain gauge array under the screen. The application also visually guides the fingertip placement and actuation and then computes BP from the measurements just like many automatic cuff devices. We tested the application, along with a finger cuff device, against a standard cuff device. The application yielded bias and precision errors of −4.0 and 11.4 mmHg for systolic BP and −9.4 and 9.7 mmHg for diastolic BP ($n = 18$). These errors were near the finger cuff device errors. This proof-of-concept study surprisingly indicates that cuff-less and calibration-free BP monitoring may be feasible with many existing and forthcoming smartphones.

Finally, we developed easy-to-understand models relating PPG waveform features to BP changes (after a single cuff calibration) and determined conclusively whether they provide added value or not in BP measurement accuracy. Stepwise linear regression was employed so as to create parsimonious models for predicting the intervention-induced BP changes from popular PPG waveform features, pulse arrival time (PAT, time delay between ECG R-wave and PPG foot), and subject demographics. The finger b-time (PPG foot to minimum second derivative time) and ear STT (PPG amplitude divided by maximum derivative), when combined with PAT, reduced the systolic BP change prediction RMSE of reference models by 6-7% ($p<0.022$). The ear STT together with the pulse width reduced the diastolic BP change prediction RMSE of the reference model by 13% ($p=0.003$). Hence, PPG fast upstroke time intervals can offer some added value in cuff-less measurement of BP changes.

This thesis is dedicated to my Mom, my sister, Jeremiah, and most importantly, Pork Chop.

ACKNOWLEDGEMENTS

I would like to thank Dr. Ramakrishna Mukkamala, for the excellent guidance and mentorship he provided. He has had an immeasurable impact on my life. I would also like to thank my committee members, Dr. Ioannis Papapolymerou, Dr. Selin Aviyente, Dr. Lik Chuan Lee, and Dr. Mi Zhang, for their valuable feedback and input during my presentations. In addition, I would also like to thank my colleagues at MSU: Mohsen Moslehpour, Mingwu Gao, Jiankin Liu, Anamd Chandrasekar, and Mohammad Yavarimanesh. Their input and the opportunity to collaborate with them has been invaluable to my research.

None of this would be possible without the immense support provided by my friends and family. My mother Ramani Natarajan and sister Krithika Natarajan have been the stable rock I needed. You nurtured the curious scientist in me for as long as I can remember and none of this would be possible without the sacrifices you have made for me. I cannot thank enough Jeremiah. You have been my confidante, a listening-ear to my rants and complaints, the boost whenever I needed it, and so much more. You also brought me into my adopted family here: Lee Ann, Theodore Lee, Grandma Vel, Grandma Donnie, and everyone else. Your constant help, support, patience, and love have helped me become better, both professionally and personally. It cannot have been easy feeding me for all these years. I will forever be grateful for taking me into your wonderful, ridiculous family. And finally, and she would say most importantly, I would like to thank Pork Chop. Your love, light, and wonderful personality have brought so much joy into my life and the lives of so many of those I care most about. You are the best, as you know, and deserve all the treats in the world.

TABLE OF CONTENTS

LIST OF TABLES

LIST OF FIGURES

INTRODUCTION

This dissertation uses in partial or in full material from the following publications for which all appropriate copyright permissions were granted:

1. Natarajan K, Block RC, Yavarimanesh M, Chandrasekhar A, Mestha LK, Inan OT, Hahn JO, Mukkamala R. PPG fast upstroke time intervals can be useful features for cuff-less measurement of blood pressure in humans. In Preparation.
2. Chandrasekhar A*, Natarajan K*, Yavarimanesh M*, Mukkamala R. An iPhone application for blood pressure monitoring via the oscillometric finger pressing method. Scientific Reports, 2018. (*equally contributing authors)
3. Natarajan K, Cheng HM, Liu J, Gao M, Sung SH, Chen CH, Hahn JO, Mukkamala R. Central blood pressure monitoring via a standard automatic arm cuff. Scientific Reports, 2017.

Cardiovascular diseases account for the largest percent of preventable morbidity and mortality worldwide [1]. Elevated blood pressure (BP), called hypertension, is the single largest risk factor for mortality from cardiovascular disease [2] and affects about a quarter of the world's adult population [3]. Hypertension can be treated with lifestyle changes and medication. Medical therapy is associated with a 35-40% reduction in the risk of stroke and a 15-25% reduction in the risk of heart disease [4]. Yet, hypertension awareness and control rates are unacceptably low [5], and deaths due to these maladies remain far too common. According to statistics from the American Heart Association, on average, someone in the US dies of cardiovascular disease (exclusive of stroke) every 40-sec and dies of stroke every 4-min [6]. Only ~55% of hypertensives in developed nations and ~45% of hypertensives in developing nations are aware of their condition, and only an abysmal ~15% of hypertensives overall have their BP under control. Ubiquitous BP monitoring technology could improve hypertension awareness by providing serial measurements from the mass population during daily life [7], and hypertension control by providing continual feedback to the individual patient [8].

Several non-invasive methods are available for monitoring BP. However, none afford anytime, anywhere measurement of BP. Auscultation is the standard clinical method [9]. This method measures systolic BP (SP) and diastolic BP (DP) by occluding the brachial artery with an inflatable cuff and detecting the Korotkoff sounds using a stethoscope and manometer during cuff deflation. The first sound indicates the initiation of turbulent flow and thus SP, while the fifth sound is silent and indicates the renewal of laminar flow and thus DP. The method requires a skilled operator.

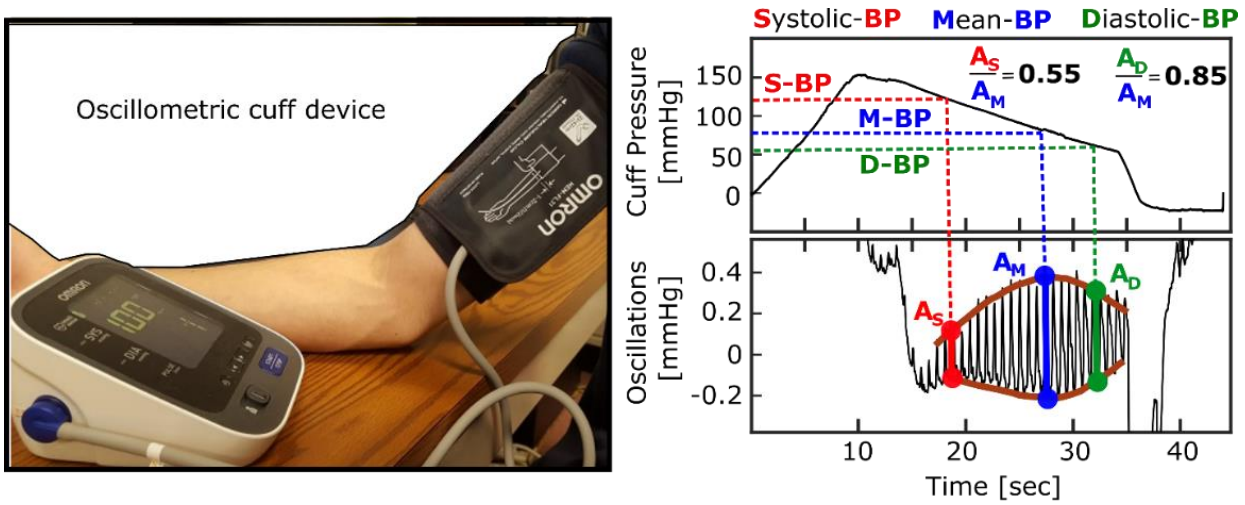

Figure 1: Conventional oscillometric BP monitoring using a cuff. Oscillometry is widely employed for automatic BP monitoring but has required a cuff. The cuff applies external pressure to an artery, and the device measures this pressure and the resulting variable-amplitude blood volume oscillations to construct an oscillogram and compute BP via population average algorithms (e.g., fixed-ratio algorithm).

Oscillometry is the most popular non-invasive and automatic method [10], [11]. This method, which is depicted in Fig. 1, measures mean BP, SP, and DP using a cuff that includes a sensor to record the pressure inside it. The cuff is placed over an artery, inflated to a supra-systolic level, and then slowly deflated to a sub-diastolic level. The cuff pressure rises and falls with inflation and deflation but also shows tiny oscillations indicating the pulsatile blood volume within the artery. The amplitude of these oscillations varies with the cuff pressure, as the arterial blood

volume-transmural pressure relationship is nonlinear. (Transmural pressure of an artery is defined as the internal pressure (i.e., BP) minus the external pressure (cuff pressure here).) The BP values are computed from the oscillogram (i.e., the oscillation amplitudes, as indicated via the vertical difference between the two orange envelopes in Fig. 1, versus the cuff pressure,) using a population average algorithm. The standard algorithm is to estimate mean BP as the cuff pressure at which the oscillogram is maximal (see A_M in Fig. 1) and SP and DP as the cuff pressures at which the oscillogram are fixed ratios of its maximal value (see A_S/A_M and A_D/A_M in Fig. 1) [10], [12], [13].

Volume clamping is a non-invasive and automatic method used in research [14], [15]. This method measures a BP waveform via a finger cuff with a photoplethysmography (PPG) sensor built-in to measure the pulsatile blood volume [16]. First, the cuff pressure is slowly increased to obtain mean BP via the oscillometric principle. Then, the cuff pressure is continually varied to maintain the "unloaded" blood volume (i.e., the blood volume at which the cuff pressure equals the mean BP) throughout the cardiac cycle via a fast servo-control system. The cuff pressure may therefore yield the finger BP waveform. This BP waveform is then typically converted to brachial BP, which is the proven cardiovascular risk factor, via an empirical algorithm [17]. However, the method is expensive.

Tonometry is another research method [18], [19]. This method measures a BP waveform by pressing a manometer-tipped probe on an artery. The probe must flatten or "applanate" the artery so that its wall tension is perpendicular to the probe. However, manual and automatic applanation have proven difficult. As a result, while the method should not require any calibration, the measured waveform has been routinely calibrated with a cuff in practice [20].

A major contributing factor to the high incidence of cardiovascular disease mortality is that the current BP measurement devices do not provide precise enough information. Oscillometry is

the most popular non-invasive and automatic method [10], [11]. However, these oscillometry devices generally algorithms based on population-averages that are less accurate in patients with atypical BP levels. Oscillometric device accuracy degrades in patients with high pulse pressure (PP = SP –DP) due to large artery stiffening, which occurs with aging and disease [12], [21]. The inaccuracy is clinically significant in that more than 45% of patients with pre-hypertension or Stage 1 hypertension and about 25% of patients with normotension and Stage 2 hypertension end up being misclassified. A patient-specific algorithm to estimate brachial BP from an oscillogram [22] was recently developed and it was shown that this algorithm can be significantly more accurate than widely used oscillometric devices [23].

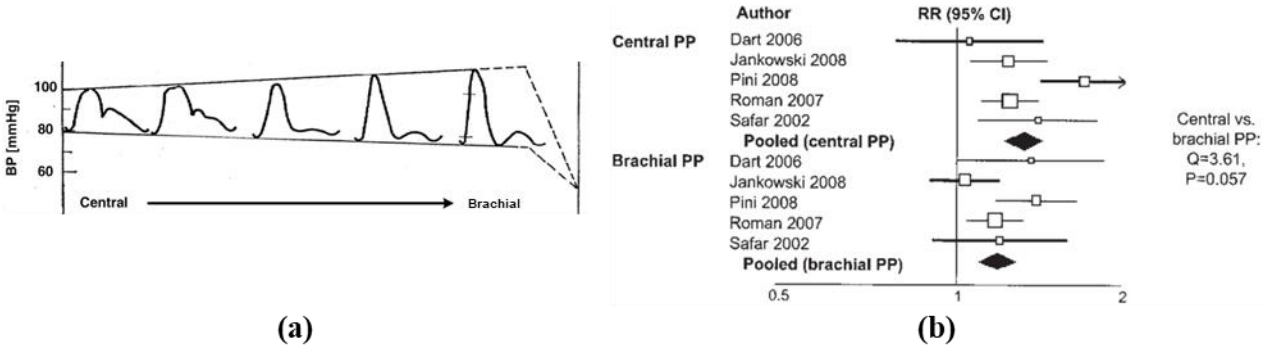

Figure 2: Central BP is more clinically relevant than brachial BP. Standard automatic arm cuff devices estimate BP at the brachial artery and not near the heart (i.e., central BP), which is more relevant. (a) Central SP (SP) and pulse pressure (PP = SP –DP) are lower than brachial SP and PP due to arterial wave reflection [11]. So, it is central BP that truly indicates cardiac performance. (b) Central BP is therefore a better cardiovascular risk stratifier than brachial BP [12].

Furthermore, standard automatic cuff devices estimate BP only at the brachial artery. However, as shown in Fig. 2a, central BP is not the same as brachial BP [24]. Most notably, central SP and PP are lower than brachial SP and PP. This well-known but counter-intuitive phenomenon is mainly caused by peripheral wave reflection in the arteries. Hence, it is central BP that truly determines cardiac performance. As a result, as shown in Fig. 2b, central BP is a better indicator of cardiovascular risk than brachial BP [25].

We developed a physiologic algorithm to estimate central BP using a standard oscillometric arm cuff device and showed – for the first time – that central BP can be measured reliably and in the exact same way as traditional brachial BP [26]. These studies were based on off-line, but blinded, analyses of previously recorded cuff pressure waveforms and invasive reference brachial and central BP measurements from patients. Successful completion of this task could ultimately help lead to reduced cardiovascular mortality and events as well as healthcare costs. This work was published in Scientific Reports [26].

Common to all these BP measurement methods is the requirement of a cuff. Cuffs are not readily available and therefore do not permit ubiquitous BP monitoring. That is, people in low resource settings may not have any access to cuff-based devices; others must go out of their way (e.g., to a pharmacy) to use these devices; and even people who own a device cannot carry it with them wherever they go. As a result, cuff-less BP monitoring devices are now being widely pursued. Pulse transit time (PTT) is the most popular method [16]. PTT often varies inversely with BP in a person and can be measured simply as the relative timing between proximal and distal waveforms indicative of the arterial pulse. Hence, PTT could potentially permit ultra-convenient BP monitoring. However, PTT in units of milliseconds must be calibrated to BP in units of mmHg, and PTT, as a single value, cannot independently track SP and DP. As a result, accuracy is the concern for the PTT-based approach. Ultrasound may allow for other methods. The most popular ultrasound method is to measure an arterial diameter waveform along with the local PTT (in the form of pulse wave velocity) and then apply the Bramwell-Hill equation to compute the absolute pulse pressure (PP = SP – DP) [27]–[29]. DP may also be measured by calibrating the measured PTT. However, ultrasound systems are generally much less convenient than automatic cuff devices.

We proposed a method for cuff-less and calibration-free BP monitoring via a smartphone using a custom PPG-force sensor unit affixed to the back of the smartphone to implement the "oscillometric finger pressing method" and showed that the device can be usable and accurate compared to cuff devices [30]. The method represents an extension of the time-honored oscillometric cuff BP measurement principle. However, the need for special sensors above and beyond the smartphone limits the accessibility of the method. Here, we developed a smartphone application that leverages PPG and force sensors already in the phone to implement the oscillometric finger pressing method. We then tested the application against cuff BP measurements for a proof-of-concept demonstration [31]. This work was published in Scientific Reports [31].

While the smartphone application implementation of the "oscillometric finger pressing method" is far more accessible and convenient than standard cuff devices while still being accurate, the drawback of this approach is that is requires user interaction to perform a measurement. Hence, it is not suitable for passive and seamless BP monitoring. PPG is a highly convenient, simple measurement of arterial blood-volume oscillations. The ease of obtaining this signal, along with the increased popularity and access to machine learning techniques, have led to an increased interest in PPG waveform analysis approaches for cuff-less BP monitoring. However, the efficacy of this data-driven approach and the useful features and models remain largely unclear. The objectives were to develop easy-to-understand models relating PPG waveform features to BP changes (after a single cuff calibration) and to determine conclusively whether they provide added value or not in BP measurement accuracy. The study data comprised finger, toe, and ear PPG waveforms, electrocardiogram (ECG) waveforms, and reference manual cuff BP measurements before and after slow breathing, mental arithmetic, cold pressor, and nitroglycerin. The data was from 32 normotensive and hypertensive humans.

Stepwise linear regression was employed so as to create parsimonious models for predicting the intervention-induced BP changes from popular PPG waveform features, pulse arrival time (PAT, time delay between ECG R-wave and PPG foot), and subject demographics. Leave-one-out cross validation was applied to compare the BP change prediction RMSEs of the resulting models to reference models in which PPG waveform features were excluded as input. The finger b-time (PPG foot to minimum second derivative time) and ear slope transit time or STT (PPG amplitude divided by maximum derivative), when combined with PAT, reduced the systolic BP change prediction RMSE of reference models by 6-7% ($p<0.022$). The ear STT together with the pulse width reduced the diastolic BP change prediction RMSE of the reference model by 13% ($p=0.003$). Hence, PPG fast upstroke time intervals can offer some added value in cuff-less measurement of BP changes. This work is in preparation and will be published.

CENTRAL BLOOD PRESSURE MONITORING VIA A STANDARD AUTOMATIC ARM CUFF

The contents presented in this chapter were originally published as:

1. Natarajan K, Cheng HM, Liu J, Gao M, Sung SH, Chen CH, Hahn JO, Mukkamala R. Central blood pressure monitoring via a standard automatic arm cuff. Scientific Reports, 2017.

Current oscillometric devices for monitoring central BP maintain the cuff pressure at a constant level to acquire a pulse volume plethysmography (PVP) waveform and calibrate it to brachial BP levels estimated with population average methods. A physiologic method was developed to further advance central BP measurement. A patient-specific method is applied to estimate brachial BP levels from a cuff pressure waveform obtained during conventional deflation via a nonlinear arterial compliance model. A physiologic method is then employed to extract the PVP waveform from the same waveform via ensemble averaging and calibrate it to the brachial BP levels. A method based on a wave reflection model is thereafter employed to define a variable transfer function, which is applied to the calibrated waveform to derive central BP. This method was evaluated against invasive central BP measurements from patients. The method yielded central SP, DP, and PP bias and precision errors of -0.6 to 2.6 and 6.8 to 9.0 mmHg. The conventional oscillometric method produced similar bias errors but precision errors of 8.2 to 12.5 mmHg ($p \leq 0.01$). The new method can derive central BP more reliably than some current non-invasive devices and in the same way as traditional cuff BP.

Introduction

Tonometric devices for non-invasive monitoring of central BP have been available for many years now. These devices either acquire a carotid artery tonometry waveform and calibrate

it with brachial cuff BP levels for a "direct" measurement of central BP or obtain a similarly calibrated, but easier-to-measure, radial artery tonometry waveform and then apply a generalized transfer function (GTF) to the peripheral BP waveform for an indirect measurement of central BP. The devices have even been shown to provide added clinical value over traditional brachial cuff BP measurements in several research studies [25]. Yet, because applanation tonometry of any artery is nontrivial, they have not reached patient care.

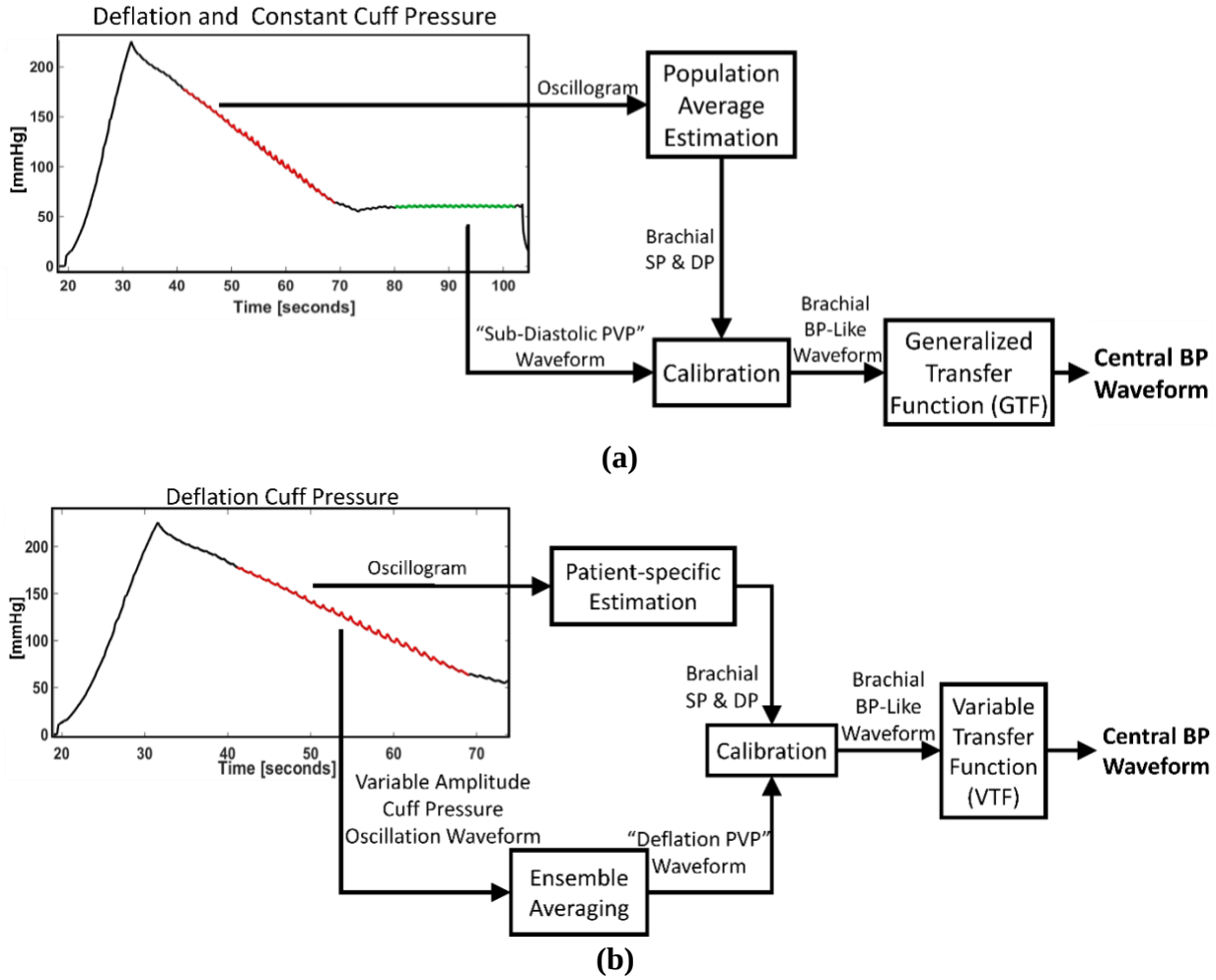

Figure 3: Conventional and physiological methods for central BP estimation. (a) Conventional method for monitoring central BP via a special automatic arm cuff device. The oscillogram is the variable cuff pressure oscillation amplitude versus cuff pressure function; PVP, pulse volume plethysmography. and (b) Physiologic method for monitoring central BP via a standard automatic arm cuff device. The sub-methods are shown in Figs. 17-19.

As a result, oscillometric devices for more convenient monitoring of central BP have recently been introduced [32], [33]. As indicated in Fig. 3a, these devices employ a special automatic arm cuff to derive central BP generally in four steps. First, brachial BP levels are obtained in the standard way by slowly deflating (or inflating) the cuff and then estimating the values from the oscillogram (i.e., the variable cuff pressure oscillation amplitude versus cuff pressure function). Second, a fixed amplitude cuff pressure oscillation or "pulse volume plethysmography (PVP)" waveform is measured by maintaining a constant cuff pressure around the DP for up to 30 sec [34]–[38] or even above the SP level by up to 35 mmHg [39], [40]. Third, a brachial BP-like waveform is derived by calibrating the PVP waveform with the brachial BP levels. Fourth and finally, central BP is computed from the peripheral waveform typically via a GTF.

The error in the measured central BP can be substantial [32]. Like the tonometric devices, the main error source is the error in the brachial BP levels used for calibration [32], [41], [42]. This latter error can be large, because automatic arm cuffs employ population average methods to estimate the brachial BP levels [10], [12], [21]. A secondary error source may be error arising from the use of a one-size-fits-all GTF.

Our broad objective is to achieve accurate central BP monitoring via a standard automatic arm cuff. In recent studies, we developed a patient-specific method for estimating brachial BP levels from the oscillogram by leveraging physiologic modeling [22] and showed that this method can be more accurate than widely used population average methods [23]. In this study, we conceived simple, yet physiologic, methods to extract the PVP waveform from the variable amplitude cuff pressure oscillation waveform and to vary the transfer function relating calibrated PVP to central BP with BP-induced changes in arterial stiffness. We then assessed the integrated

method against a high-fidelity aortic catheter in a challenging set of patients. Our results indicate that the physiologic method can derive central BP more reliably than some current non-invasive devices and in the exact same way as traditional brachial cuff BP.

Materials and Methods

Physiologic Method for Central BP Monitoring via a Standard Automatic Arm Cuff

The developed method is based on physiologic modeling and knowledge and is overviewed in Fig. 3b. This method computes the central BP waveform from a cuff pressure waveform obtained only during conventional deflation (or inflation). First, a patient-specific method is applied to an oscillogram (derived from the waveform) to yield brachial SP and DP. Then, an ensemble averaging/calibration method is applied to the variable amplitude cuff pressure oscillation waveform (obtained by high pass filtering the cuff pressure waveform) to extract a "deflation PVP" waveform and scale it to the brachial BP levels. Finally, a variable transfer function (VTF) method is employed to convert the brachial BP-like waveform to the central BP waveform. Each of the three sub-methods is described below.

Patient-Specific Method for Estimation of Brachial SP and DP

The patient-specific method is shown in Fig. 4 and described in detail elsewhere [22]. As briefly explained in [23], the oscillogram (difference between the upper and lower envelopes in red) is represented with a physiologic model accounting for the nonlinear brachial artery blood volume-transmural pressure relationship (see Eq. (1) in Fig. 4). The model parameters represent brachial SP and DP and brachial artery mechanics [*a*, *b*, *c*, *e*]. In terms of the brachial artery compliance curve (derivative of the nonlinear relationship with respect to transmural pressure), *a*

denotes the transmural pressure at which the curve is maximal; *b* and *c* indicate the width of the curve and extent of asymmetry about its maximum; and e goes with the amplitude of the curve. The parameter *e* is also determined by the reciprocal of the cuff compliance [*k*], which is assumed to be constant in accordance with experimental data.

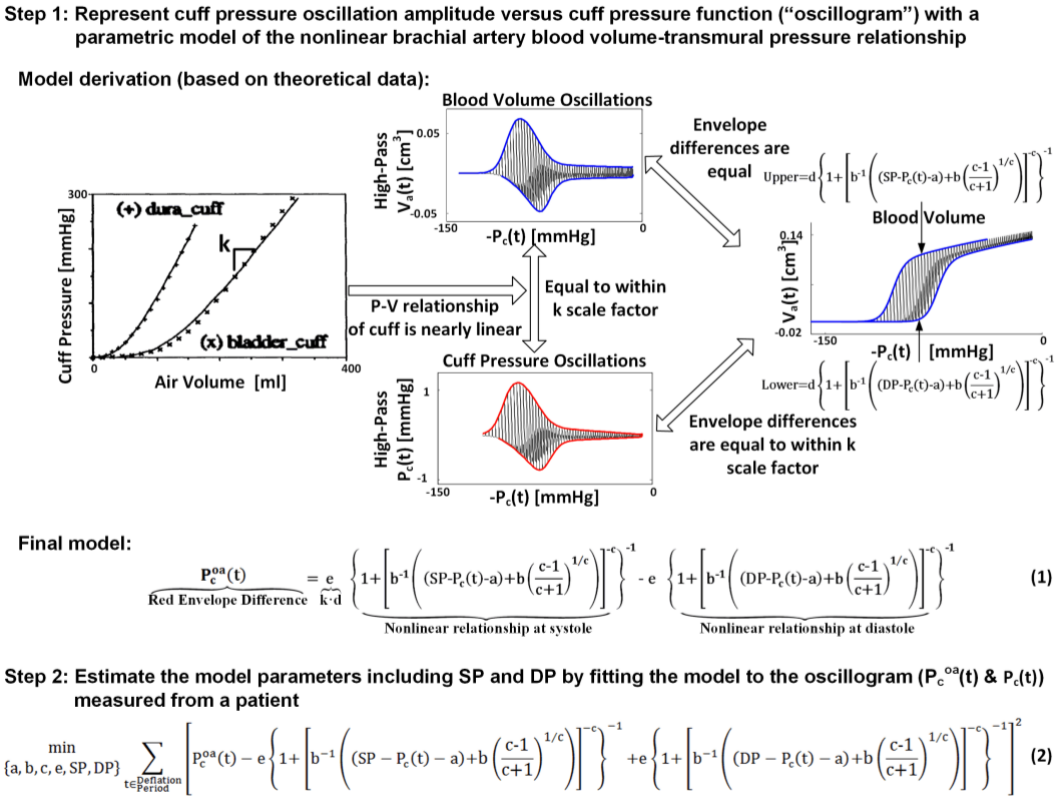

Figure 4: Overview of the patient-specific method for estimating brachial BP. Patient-specific method for estimating brachial BP levels from a cuff pressure waveform obtained during conventional deflation by leveraging a physiologic model and parameter estimation. The method is described in detail in [22]; and figure reproduced from [23].

As buttressed by directly measured compliance curves [11], a is fixed so that the curve peaks near zero transmural pressure, and b is constrained by the value of c such that the curve is right-skewed. The remaining four patient-specific parameters (i.e., brachial SP, brachial DP, c, e) are then estimated by least squares fitting of the model to the oscillogram (see Eq. (2) in Fig. 4). The user-selected variables (most notably, the a and b constraints) were established using a training dataset comprising cuff pressure waveforms for analysis and invasive reference brachial BP waveforms

from cardiac catheterization patients.

Ensemble Averaging/Calibration Method for Estimation of the Brachial BP Waveform

The patient-specific method also outputs the entire brachial BP waveform via additional steps dictated by its underlying model. While this waveform is suitable for estimating mean BP (MP), it contains artifact caused by inter-beat cuff pressure variations. Hence, another method is applied to extract a brachial BP-like waveform from the variable amplitude cuff pressure oscillation waveform. This method is simpler but still founded in physiology. Specifically, each beat of the waveform not only varies in amplitude but also in shape. The shape variations are likewise due (in part) to the brachial artery compliance changes with transmural pressure [11]. Since this compliance may be relatively constant at higher transmural pressures wherein elastin fibers play a greater role in arterial wall mechanics [16], the shape of a beat of the waveform may better reflect that of the brachial BP waveform at lower cuff pressures. Hence, a deflation PVP waveform is extracted from the variable amplitude waveform over the lower cuff pressure range via robust ensemble averaging and calibrated to the brachial BP levels.

The ensemble averaging/calibration method is shown in Fig. 5. The variable amplitude cuff pressure oscillation waveform is extracted from the minimum cuff pressure analyzed by the patient-specific method minus 40 mmHg to this minimum cuff pressure (red shading). The waveform beats are detected. To eliminate anomalies, all waveform beats of lengths within 30% of the average beat length are selected. If fewer than three waveform beats meet this criterion, then the three waveform beats with lengths closest to the average beat length are selected. Each selected waveform beat, including 250 msec intervals before the first foot and after the last foot, is equalized by normalization to peak amplitude of one and feet amplitudes of zero. (Time normalization could also be employed, if necessary, to further equalize the waveform beats.) To further eliminate

anomalies, a template waveform beat is constructed by computing the ensemble median of all selected waveform beats over the minimum beat length and then applying the same normalization. The three waveform beats with root-mean-squared-error (RMSE) < 0.5 relative to the template waveform beat that are nearest to the minimum cuff pressure are selected (red traces). If less than three waveform beats meet this criterion, then the three waveform beats with the lowest RMSEs are selected. The ensemble average of the selected waveforms beats is computed over the minimum beat length and likewise normalized to yield the deflation PVP waveform. This waveform is then scaled to brachial SP and DP to yield a brachial BP-like waveform. All user-selected variables (e.g., 30% beat length and 0.5 RMSE thresholds) were defined with a training dataset.

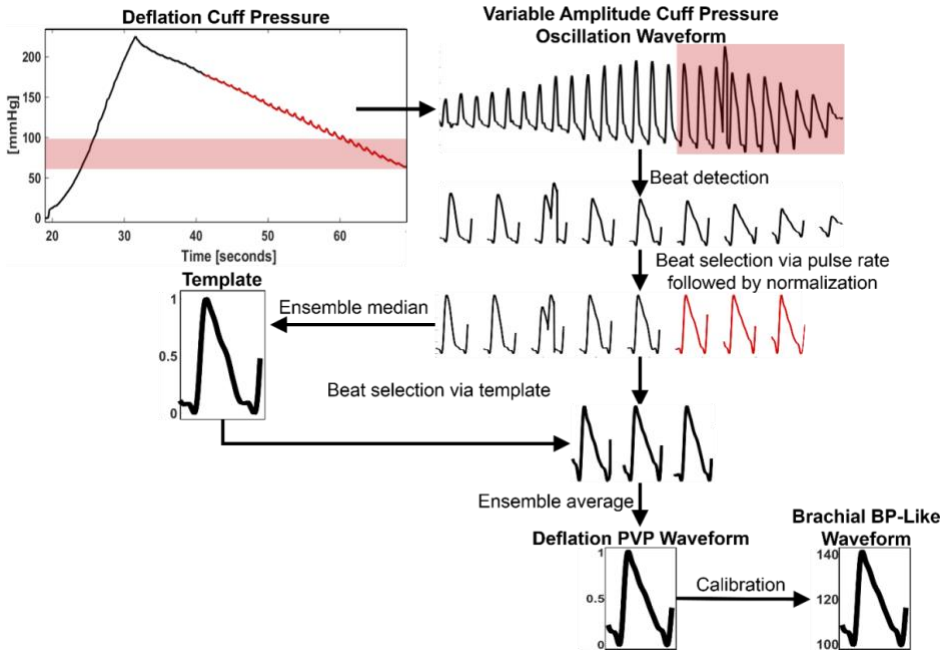

Figure 5: Overview of the ensemble averaging method for extraction of deflation PVP waveform. Ensemble averaging/calibration method for extracting a brachial BP-like waveform from the cuff pressure waveform obtained during conventional deflation. The method extracts a deflation PVP waveform by normalizing and then averaging similar waveform beats from the deflation end (wherein PVP and BP waveform shapes may better agree due to relatively constant brachial artery compliance) and then scales the waveform to brachial SP and DP.

VTF Method for Estimation of the Central BP Waveform

The VTF method is shown in Fig. 6. The method is based on a physiologic model of arterial wave reflection. This tube-load model is described in detail elsewhere [43]. Briefly, the_tube accounts for the inertance [L] and compliance [C] of the large artery segment between the ascending aorta and brachial artery and thus offers constant characteristic impedance [$Z_c = \sqrt{(L/C)}$] and permits waves to travel along it with constant pulse transit time [$T_d = \sqrt{(LC)}$]. The load accounts for the small artery resistance [R]. Waves traveling in the forward direction along the tube are reflected in the opposite direction at the terminal load with a constant reflection coefficient [$\Gamma = (R-Z_c)/(R+Z_c)$] so as to mimic the well-known amplification of brachial PP relative to central PP.

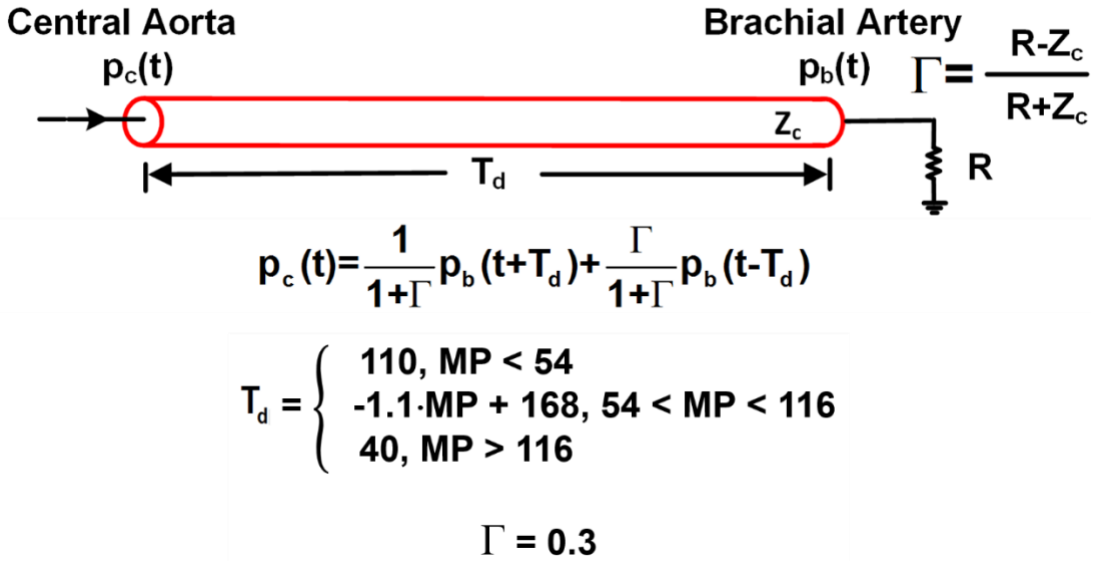

Figure 6: Variable transfer function (VTF) method for converting the brachial-like BP waveform to the central BP waveform. The method defines the transfer function in terms of the pulse transit time (T_d) and wave reflection coefficient (Γ) parameters of an arterial tube-load model and then varies T_d based on its well-known inverse relationship with mean BP (MP). MP is estimated as the time average of the brachial BP-like waveform. The model parameter values were defined via the training dataset (see Table 1). T_d is in units of msec; MP, mmHg.

According to this model, the transfer function relating the brachial BP waveform [$p_b(t)$] (i.e., BP at the tube end) to the central BP waveform [$p_c(t)$] (i.e., BP at the tube entrance) may be

defined in terms of two parameters, T_d and Γ (see transfer function equation in the time-domain in Fig. 6). As explained elsewhere [43], this transfer function is often insensitive to Γ. Hence, this parameter could be fixed to a nominal value without significantly compromising accuracy. On the other hand, T_d is a vital transfer function parameter. In particular, application of the transfer function predicts high PP amplification (ratio of brachial PP to central PP) when T_d is large and low PP amplification when T_d is small. It is well known that pulse transit time is strongly related to MP and other variables. Hence, T_d may be reasonably predicted from readily available measurements and thereby adapt to some extent to the inter-subject and temporal variations in PP amplification. The nominal value for Γ and the prediction equation for T_d were established using a training dataset (see Fig. 6). The T_d prediction equation capitalizes on the inverse relationship between pulse transit time and MP, which is due to slack collagen fibers in the arterial wall and aging [16]. This equation is simple enough that it may generally hold.

So, first, MP, computed as the time average of the brachial BP waveform over its foot-to-foot interval, is used to predict T_d. Then, the fully defined VTF is applied in the time-domain to the entire brachial BP waveform to compute the central BP waveform.

Patient Data

To investigate the physiologic method, patients admitted for diagnostic cardiac catheterization at Taipei Veterans General Hospital (Taiwan) were studied. The study procedures were approved by the hospital's IRB and conformed to the principles of the Declaration of Helsinki. Written, informed consent was obtained from each patient.

The data collection procedures are described in detail elsewhere [44], [45]. Briefly, all patients had inter-arm cuff BP differences of no more than 3 mmHg. A high-fidelity catheter with

one or two micromanometers (SPC-320 or SSD-1059, Millar Instruments, USA) was positioned in the ascending aorta and brachial artery to sequentially or simultaneously measure gold standard reference central and brachial BP waveforms.

Table 1: Measurement and Patient Characteristics

		Training	Testing	
			Cohort 1	Cohort 2
Measurements				
	Device	Microlife	Omron	Microlife
	Device measurements	deflation cuff pressure waveform + office brachial BP levels + sub-diastolic PVP waveform		
	Reference	invasive brachial and central BP waveforms		
	# of subjects	36	43	8
	# of baseline measurements	36	38	8
	# of nitroglycerin measurements	36	13	8
	# of repeated measurements	70	0	10
	Total # of measurements	142	51	26
Patients				
	Type	cardiac catheterization		
	Age [years]	64.9±12.6	57.1±13.9	71.2±12.7
	Weight [kg]	75.7±13.1	69.7±12.1	69.3±14.9
	Height [cm]	161.8±8.2	163.5±8.8	161.2±10.5
	Waist circumference [cm]	90.4±12.5	92.6±11.5	94.5±11.0
	Men [%]	75.7	75.0	75.0
	Smoking [%]	18.9	20.5	25.0
	Hypertension [%]	59.5	56.8	87.5
	Type 2 Diabetes mellitus [%]	29.7	31.8	50.0
	Dyslipidemia [%]	37.8	40.9	37.5
	Coronary artery disease [%]	59.5	56.8	62.5
	Chronic renal failure [%]	2.7	2.3	12.5
	α-Blockers [%]	13.5	11.4	25.0
	β-Blockers [%]	43.2	38.6	62.5
	Calcium channel blockers [%]	48.6	40.9	25.0
	Diuretics [%]	18.9	20.5	37.5
	Antiplatelet agents [%]	86.5	70.5	87.5

An appropriately sized, inflatable cuff of a special office device (WatchBP Office,

Microlife AG, Switzerland or VP-1000, Omron Colin, Japan) was placed over the other brachial artery to measure the cuff pressure waveform via conventional deflation, a PVP waveform via maintenance of the cuff pressure at 60 mmHg ("sub-diastolic PVP" waveform) for 30 sec, and the brachial BP levels estimated by the device. All these cuff measurements were obtained during each sequential BP waveform measurement or the simultaneous BP waveform measurement under baseline and/or sublingual nitroglycerin conditions. Repeated cuff measurements were made per condition for the Microlife device.

All sets of cuff pressure and BP measurements were screened for possible exclusion from subsequent analysis. The exclusion criteria for a measurement set were: (a) substantial artifact due to motion or otherwise in at least one waveform as determined by visual inspection; (b) MP difference in sequentially measured brachial and central BP waveforms exceeding 5 mmHg; or (c) sequentially measured BP waveforms during the transient nitroglycerin condition. The latter two criteria ensured that the central and brachial BP waveforms were indicative of the same physiologic state. About 120 patients were included for study, and a total of 209 measurement sets from 87 patients remained for analysis. The measurement sets from 36 of the patients were previously used to develop the patient-specific method for estimating brachial BP levels, so these data constituted the training dataset. The measurement sets from the other 51 patients formed the testing dataset. Table 1 shows the measurement and patient characteristics for the datasets. Note that the testing dataset included Omron and Microlife cohorts.

Data Analysis

The training dataset was analyzed to develop the physiologic method. The patient-specific method was rigorously developed as described elsewhere [22], whereas simple, but sub-optimal,

approaches were applied here to develop the ensemble averaging and VTF methods. For comparison, the training dataset was also used to build the conventional method of Fig. 3a.

To develop the ensemble averaging method, the variable amplitude cuff pressure oscillation waveforms and sub-diastolic PVP waveforms were analyzed. In particular, the user-selected variables of the method were established so that the RMSE of the deflation PVP waveform extracted from the variable amplitude waveform with respect to the corresponding sub-diastolic PVP waveform (formed by conventional ensemble averaging and amplitude normalization for the average waveform beat but not the individual waveform beats) was < 0.1.

To develop the VTF method, the sub-diastolic PVP waveforms, simultaneously measured central BP waveforms, and invasive brachial BP waveforms were analyzed. The sub-diastolic PVP waveforms were first calibrated to invasive brachial DP and SP to avoid over-fitting the transfer function to random calibration error. For each pair of brachial BP-like and central BP waveforms, Γ and T_d were estimated by least squares fitting of the model predicted central BP waveform (see Fig. 6) to the measured central BP waveform. The value of Γ was then set to the average of the Γ estimates. A T_d prediction equation was created using the T_d estimates as the dependent variable and various measurements as the independent variables. The investigated independent variables included the invasive brachial BP levels (to likewise prevent overfitting of the equation), the brachial artery compliance parameter estimates of the patient-specific method, pulse rate, and patient anthropomorphic data such as age, height, and arm circumference. Multivariate linear regression was employed, and the utility of the independent variables was assessed using a stepwise approach. MP was concluded to be the only independent variable in the final prediction equation (see Fig. 6). The correlation coefficient between the predicted and measured T_d was almost 0.6. PTT limits were thereafter added to the T_d prediction equation to protect against gross

MP estimation error (see Fig. 6).

To develop the conventional method, the averages of the aforementioned Γ and T_d estimates were employed to define a tube-load model GTF method. Note that this approach is justifiable, because the sub-diastolic (rather than deflation) PVP waveform was used and calibrated to invasive (instead of patient-specific) brachial SP and DP in the development of the VTF method. Also note that other possible implementations of the conventional method such as calibrating the sub-diastolic PVP waveform to invasive brachial DP and MP, defining the GTF using the sub-diastolic PVP waveforms calibrated to office brachial DP and SP, and building an autoregressive exogenous input GTF [43], did not improve the central BP waveform estimates in the training or even testing datasets (results not shown).

The testing dataset was then analyzed to assess and compare the accuracy of the developed methods. The physiologic method as well as the physiologic method with the VTF replaced by the GTF were applied to the standard cuff pressure waveforms, whereas the conventional method was applied to the additional, sub-diastolic PVP waveforms calibrated to the brachial SP and DP estimated by the office device from the standard cuff pressure waveforms. Note that the office devices were developed based on reference auscultation BP measurements (which underestimate invasive brachial SP and overestimate invasive brachial DP [46]). Hence, prior to PVP waveform calibration, the office brachial BP levels were adjusted so that their bias errors were the same as those of the patient-specific method for each of the two patient cohorts. This bias correction allowed the GTF to serve its intended purpose of reducing PP amplification and could easily be implemented in practice. The errors between the resulting brachial and central SP, MP, DP, and PP measurements and the gold standard reference BP levels were quantified using conventional bias [μ] and precision [σ] statistics. The bias and precision errors for the lower, middle, and upper

tertile PP amplification subgroups were also computed to investigate the added value of the VTF method. Finally, the bias and precision errors of two methods were compared via paired t-tests and Pitman-Morgan tests [47], respectively. To account for multiple comparisons, a $p \leq 0.01$ was considered significant.

Results

The training dataset was needed to develop the methods for investigation. However, the results from this dataset carry little meaning and did not offer additional insight. Hence, only the testing dataset results are provided.

Table 2: Reference BP Parameters in the Testing Dataset

	SP [mmHg]	MP [mmHg]	DP [mmHg]	PP [mmHg]	PP Amplification [unitless]
Brachial	134±21 (99 – 192)	96±13 (72 – 129)	71±11 (43 – 101)	63±19 (33 – 113)	1.2±0.15 (0.99 – 1.7)
Central	125±23 (85 – 190)	95±13 (69 – 128)	73±10 (47 – 101)	53±20 (26 – 108)	

Values are average ± SD (minimum – maximum). PP amplification is the ratio of brachial PP to central PP.

Table 3: Brachial BP Bias Errors (μ) and Precision Errors (σ) in the Testing Dataset

Method	Brachial SP [mmHg]		Brachial DP [mmHg]		Brachial PP [mmHg]	
	μ	σ	μ	σ	μ	σ
Omron	-5.7	10.7	2.7	9.5	-8.4	12.9
Patient-specific	0.7*	8.8*	3.5	7.3*	-2.8*	9.4*
Microlife	-4.5	10.6	4.4	5.4	-8.9	13.2
Patient-specific	-3.4	7.5*	-1.1*	5.8	-2.3*	10.0*

*$p \leq 0.01$ compared to corresponding office device via paired t-test for μ and Pitman-Morgan test for σ.

Table 2 shows the average±standard deviation (SD) and range of reference brachial and

central SP, MP, DP, and PP as well as PP amplification (ratio of brachial PP to central PP). All the BP parameters varied widely. Most notably, central SP and PP ranged over 105 and 82 mmHg, respectively. Table 3 shows the brachial SP, DP, and PP bias and precision errors of the patient-specific method and the office devices. The patient-specific method yielded significantly lower precision errors than the office devices and thereby afforded superior calibration. As expected, the patient-specific method also produced significantly lower bias errors. However, the office device bias errors could be corrected in practice (by e.g., adding and subtracting constant values from brachial SP and DP). Hence, in this study, the BP levels of the office devices were adjusted to make their bias errors equal to those of the patient-specific method.

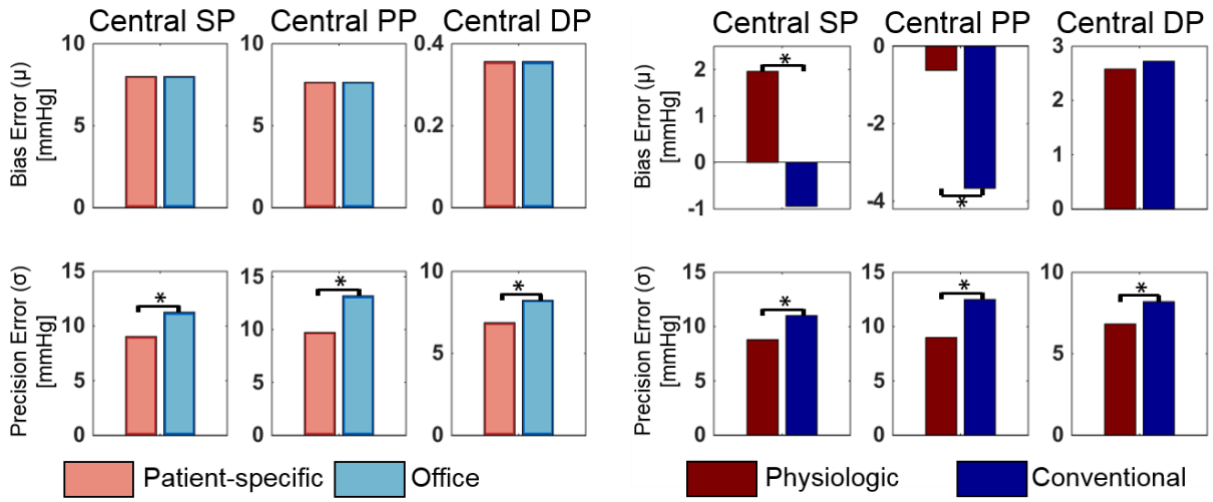

Figure 7: Central BP bias and precision errors. Central SP, pulse pressure (PP), and DP bias errors (μ) and precision errors (σ) of the patient-specific method versus the office device (a population average method) and the physiologic method versus the conventional method in the testing dataset. *$p \leq 0.01$ compared to corresponding method via paired t-test for μ and Pitman-Morgan test for σ.

Fig. 7 shows the central SP, PP, and DP bias and precision errors of the patient-specific method versus the office device (top) and of the physiologic method versus the conventional method (bottom) aggregated over both cohorts. (The precision errors for each cohort were along the lines of Table 3.) The central BP errors of the patient-specific method and office device

represent the "starting point" errors prior to applying the transfer function. As expected, the central SP and PP bias errors were large and positive. While the two methods yielded the same bias errors due to the bias correction, the patient-specific method produced significantly lower precision errors.

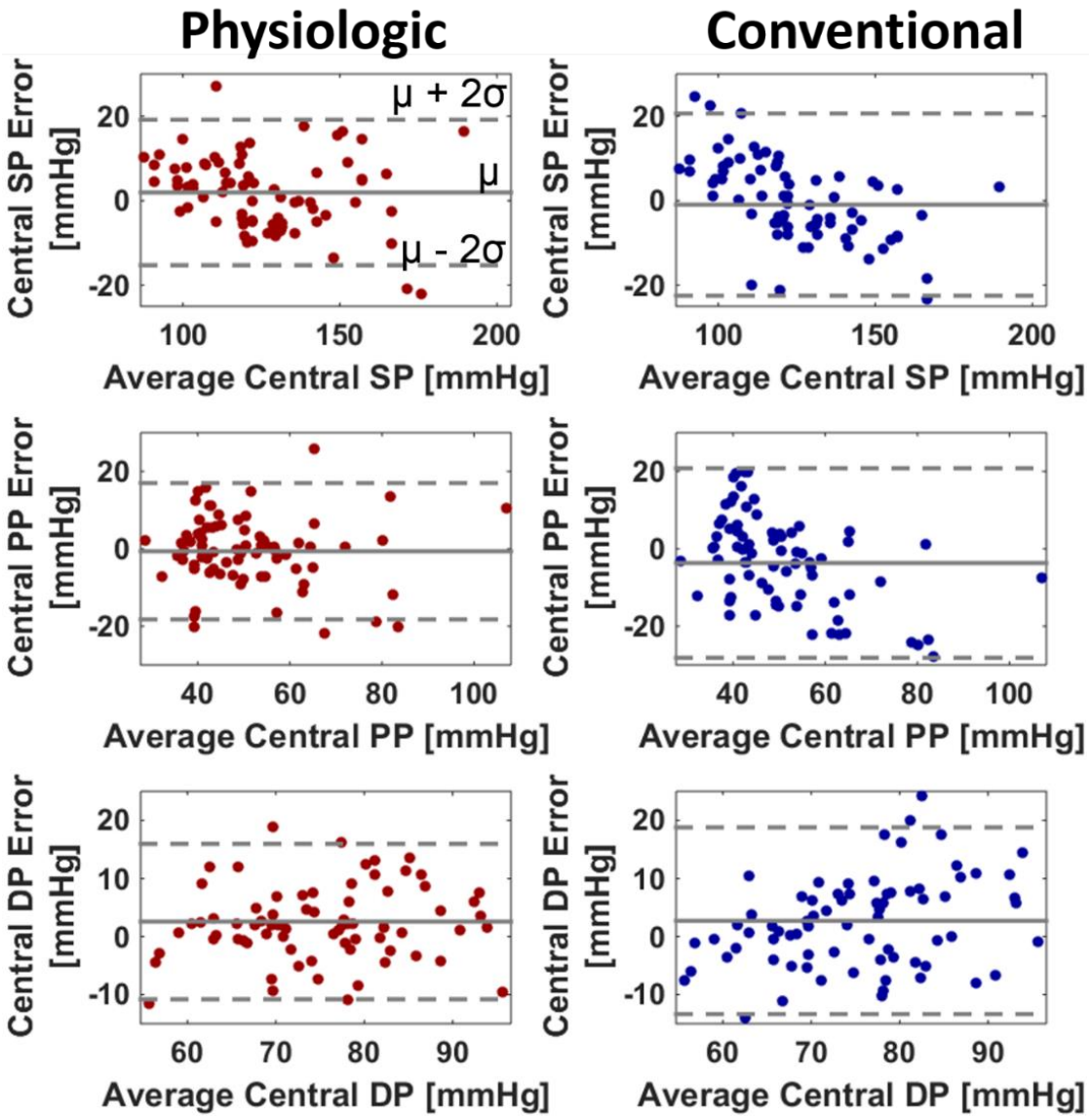

Figure 8: Bland-Altman plots of central BP errors. Bland-Altman plots of the central SP, PP, and DP errors of the physiologic method and conventional method in the testing dataset.

Comparing the precision errors to those in Table 3, it can be inferred that the main source of these errors is the calibration error rather than PP amplification variability. Application of the

transfer function reduced the central SP and PP bias errors greatly but not the corresponding precision errors (compare top to bottom). The physiologic method afforded central BP bias errors of -0.6 to 2.6 mmHg and precision errors of 6.8 to 9.0 mmHg. These errors were significantly lower than those of the conventional method by 22% in terms of average RMSE. This error reduction was mainly due to improved PVP waveform calibration.

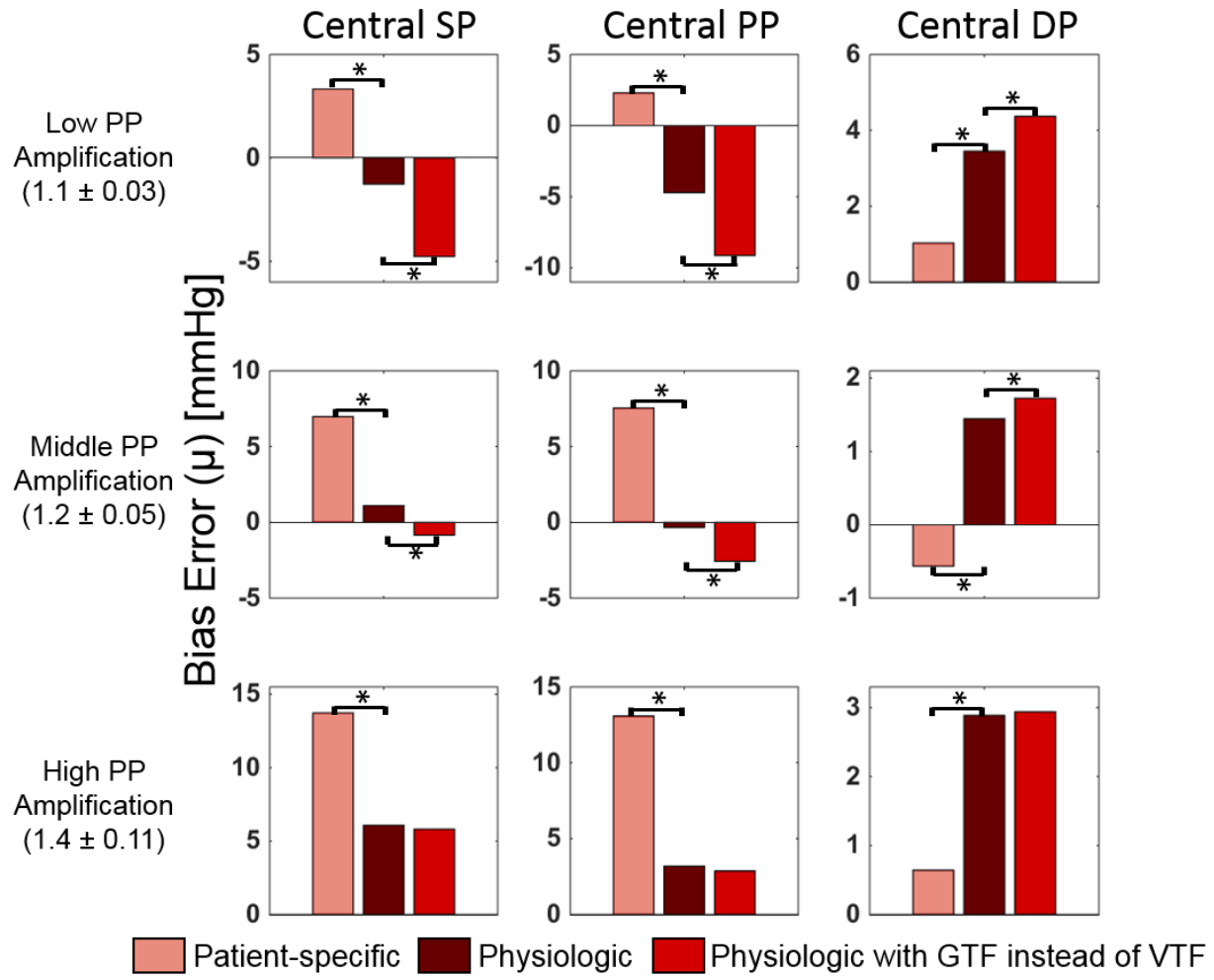

Figure 9: Bias errors of the brachial and central BP. Central SP, PP, and DP bias errors of the patient-specific method versus the physiologic method versus the physiologic method with VTF replaced by GTF for different PP amplification (ratio of reference brachial PP to central PP) subgroups in the testing dataset. *p ≤ 0.01 between physiologic method and other method via paired t-test. The precision errors of the methods were similar for the subgroups.

Fig. 8 shows Bland-Altman plots of the errors of the two featured methods for comparison.

Fig. 9 shows the central SP, PP, and DP bias errors of the patient-specific method versus the physiologic method versus the physiologic method with the VTF replaced by the GTF for the low, middle, and high PP amplification subgroups. (The precision errors were similar amongst the methods.) As expected, the patient-specific method yielded central SP and PP bias errors that were large and positive when PP amplification was high and that decreased appreciably with PP amplification. As also expected, the GTF significantly decreased the central SP and PP bias errors by mitigating the overestimation of these BP levels when PP amplification was higher but substantially increased the errors by underestimating central SP and PP when PP amplification was low. The VTF provided significantly lower central SP and PP bias errors over the whole PP amplification range by decreasing the pulse transit time parameter of the tube-load model transfer function with increasing MP. However, it was not always superior.

While the VTF reduced or maintained the central SP and PP bias errors of the GTF, its added value overall was not large due to the higher precision errors of both methods (see Fig. 7). On the other hand, the patient-specific method yielded significantly lower central DP bias errors. Hence, the patient-specific DP could instead be used to improve central DP accuracy to a mild extent. Secondary results are as follows. The ensemble averaging method yielded a RMSE of the deflation PVP waveform with respect to the corresponding sub-diastolic PVP waveform of 0.07±0.03. The time average of the deflation PVP waveform calibrated with patient-specific brachial SP and DP yielded MP bias and precision errors of 4.3 and 7.8 mmHg. Finally, the T_d prediction equation produced a correlation coefficient between predicted and measured T_d of 0.5.

Discussion

We proposed a physiologic method to monitor the central BP waveform via a standard automatic arm cuff (see Fig. 3b). First, a patient-specific method that we recently introduced [22] is employed to estimate brachial BP levels from a cuff pressure waveform obtained during conventional deflation by leveraging a physiologic model and parameter estimation (see Fig. 4). This method can yield more accurate brachial BP levels than current population average methods, as we showed previously [23] and herein (see Table 3), and may thus reduce the major calibration error of current tonometric and oscillometric devices for non-invasive monitoring of central BP [32], [41], [42]. Then, an ensemble averaging/calibration method is applied to the same cuff pressure waveform to extract a "deflation PVP" waveform and scale it to patient-specific brachial SP and DP (see Fig. 5). This simple, yet physiology-based, method may eliminate the need for the additional step performed by the available oscillometric devices in which the cuff is re-inflated to a constant pressure to measure the PVP waveform, which is then calibrated to the population average brachial BP levels (see Fig. 3a). Finally, a VTF method is employed to convert the brachial BP-like waveform to the central BP waveform. The method defines the transfer function in terms of the pulse transit time (T_d) and wave reflection coefficient (Γ) parameters of a physiologic model (see Fig. 6). The reflection coefficient is set to a nominal value, as the transfer function is often insensitive to this parameter, while the pulse transit time, which has significant impact on the extent to which the transfer function reduces PP amplification, is predicted based on its well-known inverse relationship with MP (see Fig. 6). This simple, physiologic modeling method may thus adapt the transfer function to BP-induced changes in arterial stiffness unlike the GTF, which is utilized by most of the current tonometric and oscillometric devices (see Fig. 3a). In this way, central BP could be measured – for the first time – both reliably and in the exact same way as

traditional brachial cuff BP.

We developed and evaluated the physiologic method using data from cardiac catheterization patients (see Table 1). These data included the cuff pressure waveform obtained during conventional deflation, the brachial BP levels estimated from this waveform by popular office devices, a "sub-diastolic PVP" waveform obtained during constant inflation at 60 mmHg, and gold standard invasive reference central and brachial BP waveforms. In the testing dataset, the reference BP parameters varied widely (e.g., central SP ranged from 85 to 190 mmHg) mainly due to differing degrees of patient arterial stiffness (see Table 2). The precision errors between the brachial SP and PP computed by the office device and reference central SP and PP were 11.3 and 13.2 mmHg, respectively (see Fig. 10). These high "starting point" errors together with the wide BP parameter range underscored the challenge presented by the testing dataset.

The physiologic method yielded central SP, DP, and PP bias errors within 2.6 mmHg in magnitude and precision errors within 9 mmHg (see diastolic PVP waveform calibrated with office brachial BP levels to derive the central BP waveform (see Fig. 3a) [34], [35], [38]. Since the office devices were built using auscultation rather than invasive BP as the reference and since there is systematic error between the two reference methods [46], the bias errors of the office brachial BP levels (see Table 3) were first corrected to be the same as the patient-specific method. A GTF defined by the tube-load model in Fig. 6, but with nominal values for both parameters, was then applied. Note that other possible implementations of the conventional method did not perform better.

Compared to the conventional method, the physiologic method produced significantly lower central SP, DP, and PP errors (see Figs. 13 and 14). Overall, the physiologic method yielded a 22% error reduction. The improved calibration afforded by the patient-specific method was the

main contributor to the reduction (see Table 3 and Fig. 7). The transfer function adaptation to BP-induced arterial stiffness changes offered by the VTF method was a secondary contributor and was most helpful relative to the GTF method in patients with low PP amplification (see Fig. 9) where it was able to reduce the average central BP RMSE by 10%. The VTF method did not reduce the error compared to the GTF method in patients with high PP amplification, as the T_d prediction via MP actually underestimated T_d on average. Further, the deflation PVP waveforms produced by the ensemble averaging method were similar enough to the sub-diastolic PVP waveforms that they hardly impacted the central BP errors (results not shown).

Other methods for central BP monitoring via an automatic arm cuff are available that instead obtain a supra-systolic PVP waveform and/or compute central BP from a calibrated PVP waveform without using a GTF. One method applies a transfer function based on the tube-load model in Fig. 6 to a calibrated, supra-systolic PVP waveform to derive the central BP waveform [39]. The interesting idea is that, when the brachial artery is occluded by the supra-systolic cuff inflation, the forward and backward waves will be equal in magnitude [48]. In this way, Γ is correctly determined as unity. However, the transfer function is often insensitive to Γ [43], as we have mentioned, and whether the more important T_d can be well determined from the proposed time delay between systolic PVP peaks or not is less certain. Further, the main source of error is the calibration rather than the transfer function, and the supra-systolic PVP waveform is small and thus susceptible to noise. Another method, which some of us developed, applies a multiple regression equation to several features of a calibrated, sub-diastolic PVP waveform of about 30 sec in duration to predict central SP and PP [44], [49], [50]. This equation can yield significantly smaller central PP errors than a GTF by effectively reducing the calibration error [50]. The reported precision errors of the method are also lower than those herein for the physiologic method [49],

but the patient data for evaluation were not the same. The error differences could also be explained by the fact that the central BP waveforms derived by the physiologic method were obtained from single cuff deflation measurements, whereas the central BP levels predicted by the regression method represented the average of two cuff deflation measurements. Such averaging can reduce the precision error by a factor of up to $1/\sqrt{2}$. In any case, future comparisons of the physiologic method with other methods should be performed using the same data and analyses to obtain a conclusive assessment of their relative accuracy.

Even if other methods prove more accurate than the physiologic method in head-to-head comparisons, the difference would presumably have to be large enough to justify their additional cuff inflation. Automatic arm cuffs are already cumbersome enough to use [16]. Requiring a prolonged sub-diastolic PVP waveform measurement, which could approximately double the measurement period, or a supra-systolic PVP waveform measurement, which is uncomfortable to the subject, may reduce patient compliance for using the device. Conversely, a method for measuring central BP with an acceptable level of error, but without changing the traditional measurement procedure, could increase the adoption of central BP.

This study has limitations. One limitation is that the data were not homogeneous (see Table 1). For example, two office devices (Microlife and Omron) were employed. Such heterogeneity could have added variability to our results. On the other hand, any variability introduced by the use of two devices may not have been substantial (see Table 3). Another limitation pertains to the VTF method. This transfer function neither accounts for differences in the shapes of brachial PVP and BP waveforms due to viscoelastic effects [51] nor is truly adaptive. That said, a superior transfer function method would not have made a major difference here, as the calibration error dominated. Adaptive transfer functions, such as those proposed by some of us [43], [51], [52] may

offer greater value when calibration error is not a factor such as when invasive peripheral BP waveforms are available or when calibrated radial artery tonometry waveforms are converted to likewise calibrated carotid artery tonometry waveforms.

In conclusion, PP and SP are amplified in the brachial artery relative to the central aorta. So, it is central BP that truly affects cardiac performance. Moreover, central BP rather than brachial BP is a major determinant of the degenerative changes that occur in aging and hypertension [53]. Hence, central BP could provide greater clinical value than brachial BP. While several studies have demonstrated the added value of central BP [25], the extent of the difference may be considered unsatisfying. One possible explanation is that non-invasive central BP measurements suffer from substantial error due to the error introduced by the calibration step, which can be similar in magnitude to the difference between central and brachial BP levels. Another explanation is that the tonometric devices that have long been available for non-invasive central BP monitoring are not convenient enough for central BP to be studied broadly. We introduced a physiologic method to both mitigate the calibration error and obtain central BP measurements in the exact same way as traditional automatic cuff BP measurements. We showed that this method can yield central BP measurements that agree with gold standard reference measurements to a significantly greater degree than some current non-invasive devices. Future investigations may be worthwhile to confirm the accuracy of the new method, especially in a real-time device, and apply it broadly to determine the full clinical potential of central BP.

AN IPHONE APPLICATION FOR BLOOD PRESSURE MONITORING VIA THE OSCILLOMETRIC FINGER PRESSING METHOD

The contents of this chapter were originally published as:

1. Chandrasekhar A*, Natarajan K*, Yavarimanesh M*, Mukkamala R. An iPhone application for blood pressure monitoring via the oscillometric finger pressing method. Scientific Reports, 2018. (*equally contributing authors)

We developed an iPhone X application to measure BP via the "oscillometric finger pressing method". The user presses her fingertip on both the front camera and screen to increase the external pressure of the underlying artery, while the application measures the resulting variable-amplitude blood volume oscillations via the camera and applied pressure via the strain gauge array under the screen. The application also visually guides the fingertip placement and actuation and then computes BP from the measurements just like many automatic cuff devices. We tested the application, along with a finger cuff device, against a standard cuff device. The application yielded bias and precision errors of -4.0 and 11.4 mmHg for SP and -9.4 and 9.7 mmHg for DP (n = 18). These errors were near the finger cuff device errors. This proof-of-concept study surprisingly indicates that cuff-less and calibration-free BP monitoring may be feasible with many existing and forthcoming smartphones.

Introduction

High BP is a major, modifiable cardiovascular risk factor [4], [54], yet hypertension awareness and control rates are low [5]. Ubiquitous BP monitoring could improve these rates, but existing devices require inflatable cuffs and thus do not afford such monitoring. While cuff-less BP measurement methods are being widely pursued, many of the methods require calibrations with cuff BP measurements [16], [55].

Recently, we proposed a method for cuff-less and calibration-free BP monitoring via a smartphone [30]. The method represents an extension of the time-honored oscillometric cuff BP measurement principle. The idea is for the user to serve as the actuator (instead of the cuff) by pressing her fingertip against the phone to steadily increase the external pressure of the underlying artery, while the phone, embedded with PPG and force transducers, serves as the sensor (rather than the cuff) to measure the resulting variable-amplitude blood volume oscillations and applied pressure. The phone also visually guides the finger actuation and then computes BP from the measurements just like a cuff device. We developed a device in the form of a custom PPG-force sensor unit affixed to the back of a smartphone to implement the "oscillometric finger pressing method" and showed that the device can be usable and accurate compared to cuff devices. However, the need for special sensors above and beyond the smartphone limits the accessibility of the method.

Here, we developed a smartphone application that leverages PPG and force sensors already in the phone to implement the oscillometric finger pressing method. We then tested the application against cuff BP measurements for a proof-of-concept demonstration.

Materials and Methods

We performed two sets of human studies under protocols approved by the Michigan State University Institutional Review Board and in accordance with relevant guidelines and regulations. We obtained written, informed consent from each subject. The purpose of the first study was to develop the iPhone application and a method for estimating the finger pressing contact area. The purpose of the second study was to conduct a proof-of-concept evaluation of the application against cuff devices. Note that the application did not output BP or a try-again message in real

time for the sake of convenience (as the BP computation algorithm of our previous device was implemented as an Android application [30] instead of an iOS application needed here). We thus applied the code for the BP computation algorithm of the previous device off-line to the finger measurements from the application while blinded to the cuff BP measurements.

Application Development

We studied 22 healthy subjects (age, 27±3 years; height, 169±12 cm; weight, 73±11, kg; 45% females). For each subject, we took two or three measurements of the fingertip "rectangular box" width (w) and height (h) via the application and three fingerprints via an inkpad and graph paper. For each fingerprint, the subject pressed firmly and uniformly in the normal direction. We averaged the w (mm) and h (mm) measurements and computed the reference finger pressing contact area (A, mm^2) as the average of the number of squares of fingerprint ink on the graph paper that were 2.7 mm (distance from the camera center to the screen edge) above the middle of the fingertip (see rationale in Results). We plotted A versus each of w, h, and w·h. After excluding two outlier data points, each set of 20 data points appeared to be well fit by a line. We found that A was best predicted from w·h (see line formula presented under Results).

Application Testing

Experimental Protocol

We studied 20 different subjects (age, 33±10 (18-55) years; height, 169±7 cm; weight, 66±10, kg; 45% females). This number of subjects is congruent with many other published studies on cuff-less BP measurement [16]. We recruited most of these subjects from the cohort employed for testing our previous device [30]. Sixteen of the subjects had never used the iPhone application,

whereas the other four subjects were experienced users of the application. The inclusion criteria were: (i) ages 18 to 60 years and (ii) normotensive or hypertensive. The exclusion criteria were (i) cardiovascular disorders other than hypertension or (ii) problems with fine motor control.

We commenced study of each subject by making the same measurements as the first human study. However, in this evaluation study, the application estimated the finger pressing contact area by applying the average of the w and h measurements to the line formula. For the new users, we then gave demonstrations on how to use the application to make finger measurements. We allowed them to perform three to six practice trials. We concluded study of each subject with a series of measurements as follows. We obtained three reference BP measurements via a standard oscillometric arm cuff device (BP786, Omron, Japan). We then had the new users make four finger measurements with the iPhone application and the experienced users make two finger measurements while holding the phone well below heart level to raise BP. We next measured the brachial BP waveform with a finger cuff device based on the volume-clamp method (Finometer Model 2, Finapres Medical Systems, The Netherlands). We thereafter obtained two more reference BP measurements using the standard cuff device. We also had the experienced users make two more measurements while holding the phone at heart level later.

Data Analysis

We applied the same code employed by our previous device [30] off-line to compute brachial BP from the entire finger blood volume oscillation and pressure recordings from the application or output a try-again message. We documented the number of BP measurements and try-again messages. We averaged all BP measurements from the iPhone application for each new user and each experienced user holding the device below the heart and averaged the last four BP

measurements from the arm cuff device. For the experienced users, we added a ρgh measurement provided by the finger cuff device (where ρ is the known blood density (near that of water), g is gravity, and h is the vertical distance between the heart and device) to the SP and DP measurements of the reference arm cuff device. We also likewise measured the reference finger pressing contact area via the fingerprinting.

As in our previous study [30], we used standard analyses to assess the SP and DP measurements from the iPhone application as well as the finger cuff device, each against the reference BP measurements from the arm cuff device. We assessed accuracy qualitatively in terms of correlation and Bland-Altman plots and quantitatively in terms of the correlation coefficient (r), bias error (μ, mean of the errors), and precision error (σ, standard deviation of the errors). We also assessed BP measurement repeatability via the mean absolute difference of successive measurements at heart level per subject in mmHg and evaluated the finger pressing contact area estimates via the mean absolute difference relative to the reference measurements in percent. Note that we only assessed the repeatability of BP measurements made with the iPhone at heart level, as it was not easy to perform BP measurements with the device well below the heart.

Results

iPhone Application

Fig. 1 illustrates the oscillometric cuff BP measurement principle, and Fig. 10a shows the application developed to extend the principle to measure BP with the latest iPhone (X model). The front of this phone is all screen, except for a small notch that includes the camera for taking "selfies". The application employs this front camera as the PPG sensor where the light source is ambient light and/or screen light (bright setting, which we anecdotally found to suffice in the dark).

Spatial averaging followed by band-pass (1.8-4.3 Hz) filtering of the red video channel is applied to extract the blood volume oscillations.

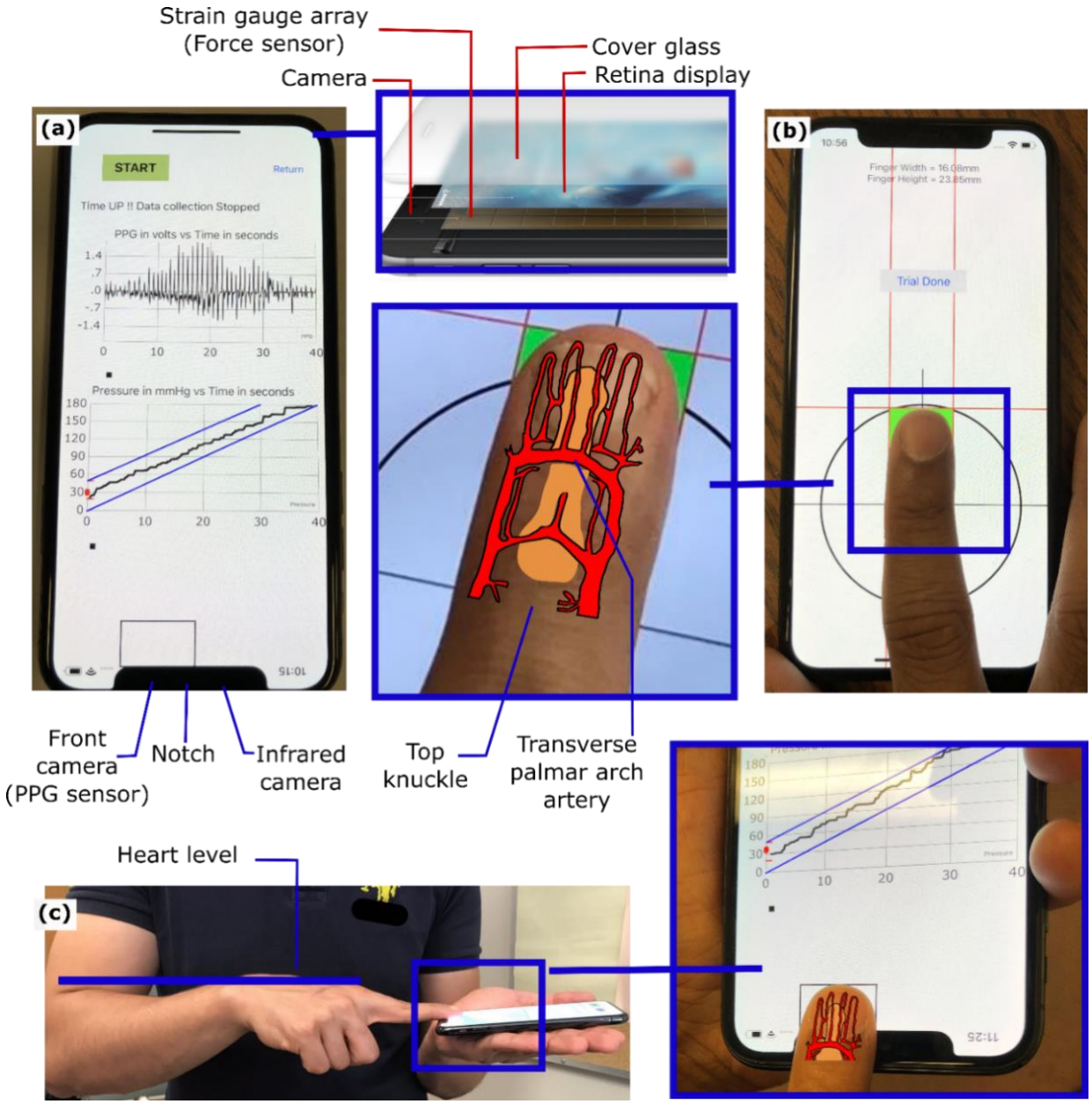

Figure 10: iPhone application implementation of the oscillometric finger pressing method for BP measurement. (a) Photograph of an iPhone X application to implement the "oscillometric finger pressing method" by measuring finger pressure via the strain gauge array under the screen and finger blood volume oscillations via the front camera. Reproduced from reference [56]. **(b)** Photograph of a user initializing the application by measuring fingertip width and height from the top of the fingertip to the artery near the middle of the fingertip. **(c)** Photograph of the user making a measurement by placing the fingertip within a rectangular box of the measured width and height; holding the phone horizontally at heart level while resting the fingertip flat on the phone; and pressing to increase the pressure within the two target blue lines.

The application employs the strain gauge array under the sphone screen (but not the notch) for employing “peek and pop” via “3D Touch” [56] as the force sensor. Apple’s UIKit is used to extract the strain gauge output [57]. Through placement of high density weights on the screen adjacent to the camera, the application derives force (F, grams) from the strain gauge output (V) as F=443.75V, where V takes on 400 levels from 0 to 0.83 (firm setting). Like our previous device [30], the application plots the data as they are recorded to visually guide the finger actuation.

Fig. 10b shows that the application also includes measurement of the user fingertip dimensions. One purpose of this measurement is to guide fingertip placement on the screen when measuring BP such that the underlying transverse palmar arch artery (at about the middle of the fingertip) is above the camera. Another purpose is to estimate the finger pressing contact area on the screen, which is needed to compute finger pressure as force divided by area. This measurement need only be made once per user, as finger dimensions and pressing contact area hardly change throughout adulthood [58]. Based on a training dataset comprising index fingertip width and height measurements via the application and reference finger pressing contact area measurements via fingerprinting from 20 subjects, the screen finger pressing contact area (A, mm^2) is calculated as $A=0.56w \cdot h-5.67$, where w and h are specifically the fingertip width at the base of the nail and half the height of the fingertip starting from the crease at the top knuckle minus 2.7 mm (distance from the camera center to the screen edge). Note that the fingerprints were obtained during firm pressing and may thus be valid around the maximum blood volume oscillation regime, which includes mean BP and is mainly used for BP computation [22]. Based on fingerprint dimensions from thousands of subjects [58] and the force measurement specifications above, we estimate that 95% of people could achieve finger pressure at maximum of >178 mmHg and resolution of <2 mmHg with the application. These specifications are largely congruent with BP measurement.

Usage

The user initializes the application by placing her index fingertip so that the crease at the top knuckle is aligned with the black horizontal line (Fig. 10b). The user or another person then moves the red vertical and horizontal lines to measure the fingertip width and height (Fig. 10b). The user may then measure BP, as shown in Fig. 10c. The user places her fingertip so that it is tightly encompassed by the rectangular box of width w and height h near the camera when viewing from directly above; holds the phone horizontally at heart level while resting her fingertip flat on the phone for uniform, normal direction force application; and presses to keep the finger pressure within the target blue lines until enough data have been obtained. Using the algorithm employed by our previous device [30], brachial BP is then computed from the finger measurements or a try-again message is outputted.

Accuracy

We tested the iPhone application in 20 different subjects. These users were mainly from the cohort employed for testing our previous device (to facilitate comparisons) and included four experienced users of the application. Each new user performed three to six practice trials followed by four measurements. Each experienced user performed two measurements holding the phone well below heart level to raise BP and two normal measurements.

The application yielded BP in about half the measurements for the new users and outputted BP in 18 of the users. However, the application did not yield BP in the other two users due to poorly estimated finger pressing contact area (29-43% error relative to fingerprinting compared to <7% mean absolute error in the 18 subjects). The BP measurements from each new user and

experienced user holding the device below the heart were averaged and assessed against BP measurements from a standard arm cuff device.

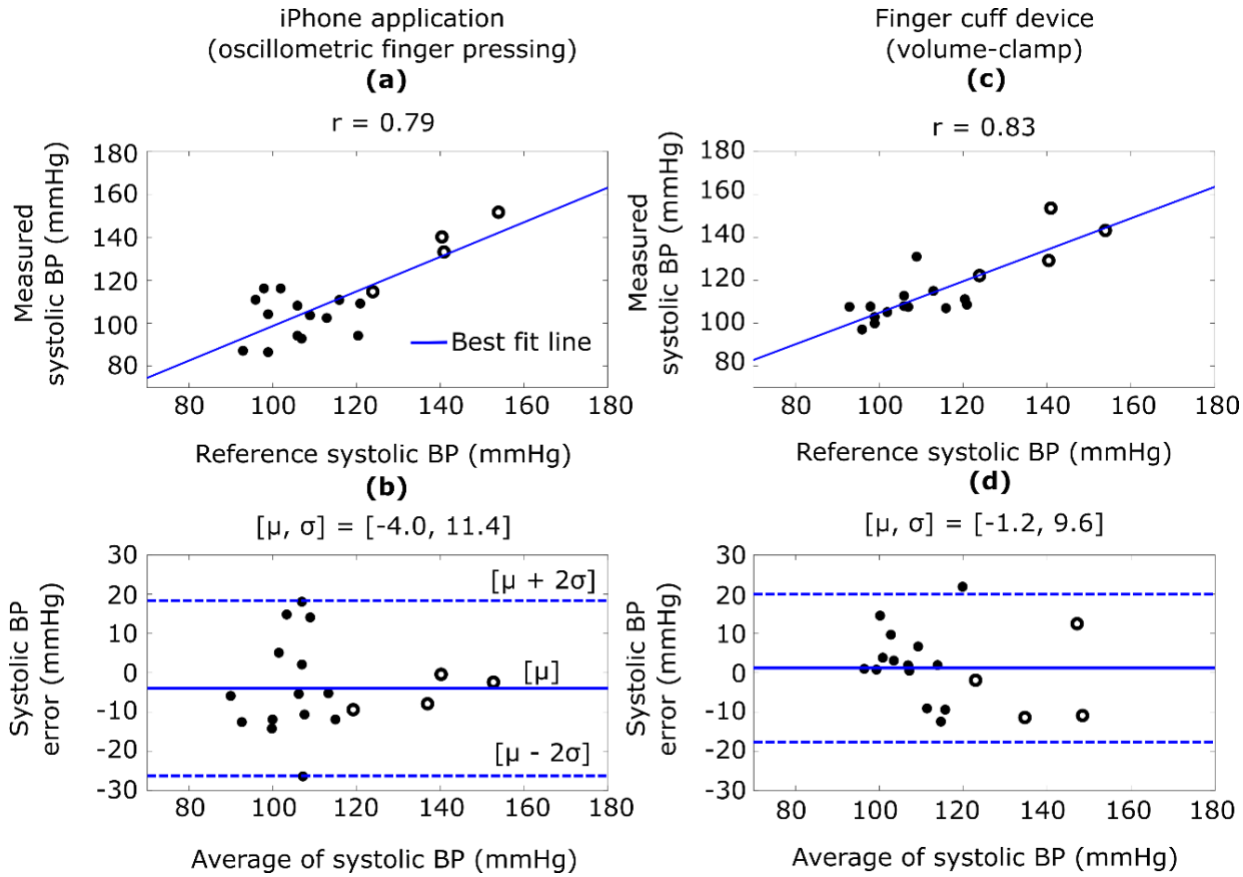

Figure 11: Bland-Altman and scatter plots of BP estimation errors. Application accuracy results (n = 18 users). Correlation and Bland-Altman plots comparing the brachial SP measurements from the (a)-(b) iPhone application and (c)-(d) a finger cuff device to those from a standard arm cuff device. The closed circles are data from new users holding the finger devices at heart level, and the open circles are data from experienced users holding the finger devices below the heart to increase BP. r, correlation coefficient; μ, mean of errors (bias error); σ, standard deviation of errors (precision error).

Fig. 11a-b shows correlation and Bland-Altman plots for the SP measurements from the 18 users. The bias errors (μ) and precision errors (σ) of the application were -4.0 and 11.4 mmHg for SP over about a 50 mmHg range of BP. Fig. 11c-d shows corresponding plots for a finger cuff device, which is FDA-cleared for measuring brachial BP [59]. The application showed errors that were only about 2 mmHg higher on average than the finger cuff device.

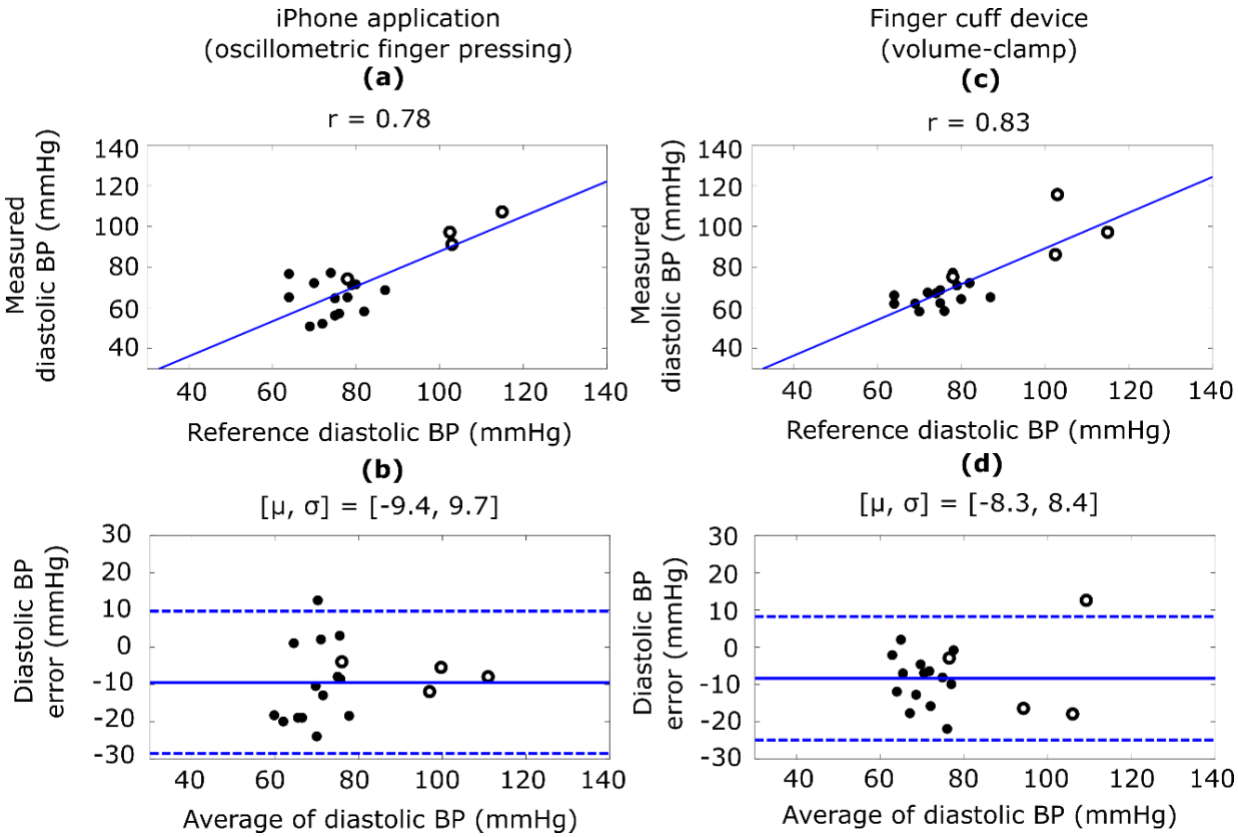

Figure 12: Application accuracy results (n = 18 users). Correlation and Bland-Altman plots comparing the brachial DP measurements from the (a)-(b) iPhone application and (c)-(d) a finger cuff device to those from a standard arm cuff device. The closed circles are data from new users holding the finger devices at heart level, and the open circles are data from experienced users holding the finger devices below the heart to increase BP. r, correlation coefficient; μ, mean of errors (bias error); σ, standard deviation of errors (precision error).

Fig. 2a-b shows correlation and Bland-Altman plots for the SP measurements from the 18 users. The bias errors (μ) and precision errors (σ) of the application were -4.0 and 11.4 mmHg for SP and -9.4 and 9.7 mmHg for DP over about a 50 mmHg range of BP. Fig. 2c-d shows corresponding plots for a finger cuff device, which is FDA-cleared for measuring brachial BP [59]. The application showed errors that were only about 2 mmHg higher on average than the finger cuff device.

Discussion

The iPhone application errors are close to our previous device [30]. However, the

application did not yield BP in two users due to finger pressing contact area mis-estimation, which is not a factor for the device. The application also yielded more try-again messages (about 50 versus 40%) and less repeatable BP measurements (e.g., mean absolute difference between successive measurements at heart level of about 7 versus 5 mmHg) likely due to variability in fingertip positioning despite the rectangular box guide. Hence, not surprisingly, the application may be less effective than our device, which employs application-specific sensors.

However, any reduction in effectiveness may be offset by the increased accessibility of a smartphone application. An estimated 50 million iPhone X models have already been sold [60]. Moreover, other smartphones have 3D Touch capability including iPhone models 6S and higher [56] and the Huawei Mate S model [61]. Hence, applications for these phones may likewise be developed (with appropriate modifications for differing arrangements of the camera/PPG sensor and screen). In 2017, 328 million iPhones with 3D Touch capability (excluding iPhone 8 and X) were being used [62]. Hence, it is conceivable that the oscillometric finger pressing method could reach about 500 million smartphones already in use.

Our iPhone application should be improved. Most importantly, the finger pressing contact area was mis-estimated in two subjects and variably estimated in some other subjects due to fingertip mis-positioning. In practice, when the application consistently outputs try-again messages or unusual BP measurements, the area could be determined with just one cuff BP measurement (as opposed to periodic cuff calibrations required by competing methods [16], [55]). The application could also output a running average of the past several BP measurements (instead of individual BP measurements) to mitigate random variability resulting from fingertip mis-positioning and other factors [55]. In this way, the application may be able to yield BP errors that are closer to the putative bias and precision errors limits of 5 and 8 mmHg [63] than the results

reported herein. However, there may be better solutions. One possibility is to measure the area (even at different finger pressures) via the fingerprint sensor under the screen for authentication in upcoming smartphones including the 2019 iPhone X [64]. The optimal solution is if Apple were to provide access to an accurate area measurement as the user performs the actuation via the capacitive sensor array also under the screen [56]. Such access may be possible, as superior area assessment may be obtained with Android devices [65]. In addition, the infrared camera also on the notch of the iPhone X (Fig. 10a) for authentication may be used to provide higher-fidelity blood volume oscillations in cold and other low signal conditions [66]. Finally, the BP computation algorithm needs further development to satisfy the accuracy requirements of a regulatory test [63].

In summary, this proof-of-concept study surprisingly indicates that cuff-less and calibration-free BP monitoring may be feasible with many existing and forthcoming smartphones by leveraging sensors built-in for other purposes. Such ubiquitous BP monitoring may improve hypertension awareness and control rates and thereby help reduce the incidence of cardiovascular disease and mortality.

PPG FAST UPSTROKE TIME INTERVALS CAN BE USEFUL FEATURES FOR CUFF-LESS MEASUREMENT OF BLOOD PRESSURE CHANGES IN HUMANS

The content of this chapter is pending publication as:

1. Natarajan K, Block RC, Yavarimanesh M, Chandrasekhar A, Mestha LK, Inan OT, Hahn JO, Mukkamala R. PPG fast upstroke time intervals can be useful features for cuff-less measurement of blood pressure in humans. In Preparation.

PPG waveform analysis is being increasingly investigated for continuous, non-invasive, and cuff-less BP measurement. However, the efficacy of this data-driven approach and the useful features and models remain largely unclear. The objectives were to develop easy-to-understand models relating PPG waveform features to BP changes (after a single cuff calibration) and to determine conclusively whether they provide added value or not in BP measurement accuracy. The study data comprised finger, toe, and ear PPG waveforms, electrocardiogram (ECG) waveforms, and reference manual cuff BP measurements before and after slow breathing, mental arithmetic, cold pressor, and nitroglycerin. The data was from 32 normotensive and hypertensive humans.

Stepwise linear regression was employed so as to create parsimonious models for predicting the intervention-induced BP changes from popular PPG waveform features, pulse arrival time (PAT, time delay between ECG R-wave and PPG foot), and subject demographics. Leave-one-out cross validation was applied to compare the BP change prediction RMSEs of the resulting models to reference models in which PPG waveform features were excluded as input. The finger b-time (PPG foot to minimum second derivative time) and ear slope transit time or STT (PPG amplitude divided by maximum derivative), when combined with PAT, reduced the systolic BP change prediction RMSE of reference models by 6-7% ($p<0.022$). The ear STT together with the pulse width reduced the diastolic BP change prediction RMSE of the reference model by 13% ($p=0.003$).

Hence, PPG fast upstroke time intervals can offer some added value in cuff-less measurement of BP changes.

Introduction

PPG is a simple yet effective technique for measuring pulsatile blood volume changes in small arteries. Since blood volume is related to BP, PPG waveform analysis is believed to be a potential approach for achieving continuous, non-invasive, and cuff-less BP measurement (typically in between periodic cuff measurements). PPG waveform analysis is more convenient than the PTT approach [16], which nominally requires two sensors for measurement. Alternatively, it can be combined with PTT, which is often detected via a PPG waveform, to seamlessly improve its accuracy.

However, unlike PTT, PPG waveform analysis for BP measurement may have little theoretical basis. The Kelvin-Voigt model of viscoelasticity, which is profound in small arteries [16], provides a simple relationship between the AC components of same site BP and PPG waveforms in the frequency-domain ($\Delta P(\omega)$ and $\Delta V(\omega)$) as follows:

$$\Delta V(\omega) = \frac{1}{j\omega\eta + E}\Delta P(\omega),$$

where E and η are the elastic modulus and coefficient of viscosity of the arterial wall [67]. The transfer function here is a lowpass filter with gain of $1/E$ and cutoff frequency of E/η. Hence, the PPG waveform is a lowpass filtered version of the BP waveform. In this way, the PPG waveform is embedded with BP information. However, the lowpass filter changes with BP variations and smooth muscle contraction, which is modulated by the brain on the time scale of seconds and can occur independently of BP changes [16]. So, for example, the PPG amplitude can vary with BP or

viscoelastic parameters. For this reason, as shown in Fig. 13, the PPG amplitude has little value in predicting BP changes during different physiologic interventions [68].

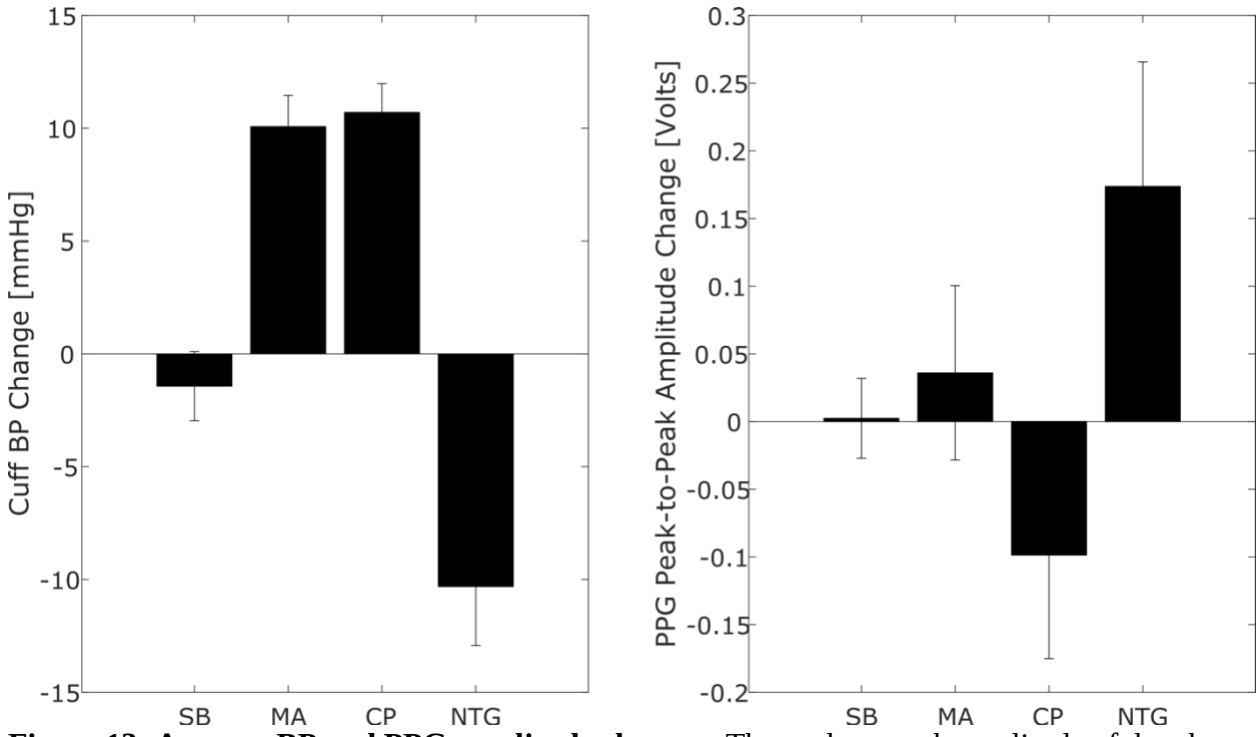

Figure 13: Average BP and PPG amplitude changes. The peak-to-peak amplitude of the photoplethysmography (PPG) waveform does not track intervention-induced blood pressure (BP) changes [68]. SB is slow breathing; MA, mental arithmetic; CP, cold pressor; and NTG, nitroglycerin. Bars are mean±standard error (SE).

Nevertheless, PPG waveform analysis for cuff-less BP monitoring is being increasingly investigated [69]–[75] due to its ultra-convenience and the current era of data-driven, machine learning. However, the accuracy of this approach, especially in terms of added value over demographic and other basic information or PTT, and the useful features and models relating the features to BP remain largely unclear. Knowledge of useful features is particularly important given that a rigorous theory may be lacking. Furthermore, many of the studies have not invoked diverse interventions to change BP [73]–[75], which is crucial for assessing the more viable "cuff-

calibrated, cuff-less" approach, or have used surgery or intensive care data [69], [70], which include challenging BP changes but may not be germane to interesting hypertension applications.

We investigated PPG waveform analysis in terms of tracking BP changes induced by a battery of diverse BP interventions in normotensive and hypertensive human volunteers. We specifically aimed to create readily interpretable models relating PPG waveform features to BP changes and to determine conclusively whether they provided added value or not in BP measurement. The models that we reveal with accompanying results herein suggest that PPG fast upstroke time intervals can offer some added value in cuff-less measurement of BP changes.

Materials and Methods

We analyzed physiologic data that we previously collected from human subjects. Our overall approach was to apply stepwise linear regression to create models for predicting intervention-induced BP changes from popular PPG waveform features, PTT, and demographics and use leave-one-out cross validation to compare the BP change prediction errors of the resulting models to reference models in which PPG waveform features were excluded as input. Physiologic data was collected from human subjects under a protocol approved by, and in accordance with the relevant guidelines and regulations of, the Institutional Review Boards of University of Rochester and Michigan State University. All subjects gave written, informed consent prior to their participation in the study.

Human Physiologic Data

We described the human physiologic data for study in detail previously [68]. Briefly, we performed the procedures under IRB approval and with written, informed consent from the

subjects. We recorded finger, toe, and ear PPG waveforms, an ECG waveform, and manual cuff BP before and after slow breathing (SB), mental arithmetic (MA), a cold pressor test (CP), and sublingual nitroglycerin (NTG, for the majority of subjects). As shown in Fig. 14, these interventions increased or decreased systolic and diastolic BP (SP and DP) to varying extents via distinct physiologic mechanisms.

We extracted 214 sets of the four waveform segments with minimal artifact and reference cuff BP values from 32 subjects (see characteristics in Results) for analysis. We previously analyzed these data to compare conventional PTTs as markers of BP and found that the best correlation by a significant extent was between toe pulse arrival time (PAT), which is the time delay between the ECG R-wave and toe PPG trough or foot, and SP (subject average r = -0.63±0.05) [68].

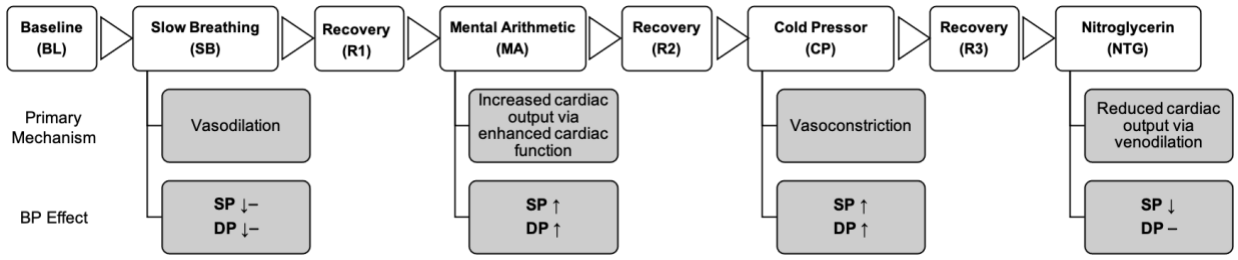

Figure 14: The subjects underwent a battery of interventions to change their BP. A battery of challenging interventions were employed to change BP differently via distinct physiologic mechanisms [76]–[79]. SP and DP are systolic and diastolic BP. Periods of recovery were included before each intervention to obtain a starting-point measurement for each intervention. Slow breathing and nitroglycerin produced decreases in BP while mental arithmetic and cold pressor increased BP.

Data Analysis

We further analyzed the data to determine if incorporating PPG waveform features could improve the tracking of the intervention-induced BP changes. Our strategy for this data-driven investigation was to employ methods intended for when the number of subjects is not high.

Pre-Processing

We first applied bandpass filters with cutoff frequencies of 0.5 and 6 Hz to the finger and toe PPG waveforms and 0.5 and 9 Hz to the ear PPG waveform. These cutoff frequencies represented a good trade-off between removing noise and retaining features. We detected the peaks of the PPG waveform via ECG-gating and then the waveform feet using the intersecting tangent method [16]. After subtracting the amplitude at the leading foot of each PPG waveform beat from the entire beat, we computed the median of the leading foot to lagging foot time interval, amplitude and timing of the peak, and amplitude of the lagging foot of each beat in a segment. We selected the five beats with features closest to the median values for the segment.

Feature Extraction

We limited the candidate PPG waveform features to popular or promising ones. Fig. 15 shows the 31 candidate features that we considered. The amplitudes, timings, and areas of the PPG waveform and its first and second derivatives are perhaps the most widely studied [80], while "slope transit time (STT)" has been shown to be inversely correlated with BP during respiratory maneuvers [81]. While other features were also used in literature, many were not well-defined or did not always exist, even in a PPG waveform of high signal quality. We also detected ear, finger, and toe PAT as the time delay between the ECG R-wave and the PPG waveform foot as another waveform feature that would also require an ECG measurement. We extracted all of these features from each of the five beats of a segment and then took the mean of the three middle values for each feature.

Type	Features
Time Intervals	$PW = t_{Foot2} - t_{Foot1}$ $t_{Peak} - t_{Foot1}$ t_a, b-time = t_b, t_c, t_d, t_e, t_f $t_{Peak} - t_f$ $(t_{Peak} - t_f)$/Subject Height $STT = Amp_{Peak}/Amp_p$
Amplitudes	Amp_{Peak} Amp_a, Amp_b, Amp_c, Amp_d, Amp_e, Amp_f Amp_b/Amp_a, Amp_a/Amp_c, Amp_a/Amp_d, Amp_a/Amp_e $(Amp_b - Amp_c - Amp_d - Amp_e)/Amp_a$ $(Amp_b - Amp_e)/Amp_a$ $(Amp_b - Amp_c - Amp_d)/Amp_a$ $(Amp_c + Amp_d - Amp_b)/Amp_a$ Amp_{DN} Amp_{DP} $(Amp_{Peak} - Amp_{DP})/Amp_{DP}$
Areas	A1+A2+A3+A4 (A3+A4)/(A1+A2)

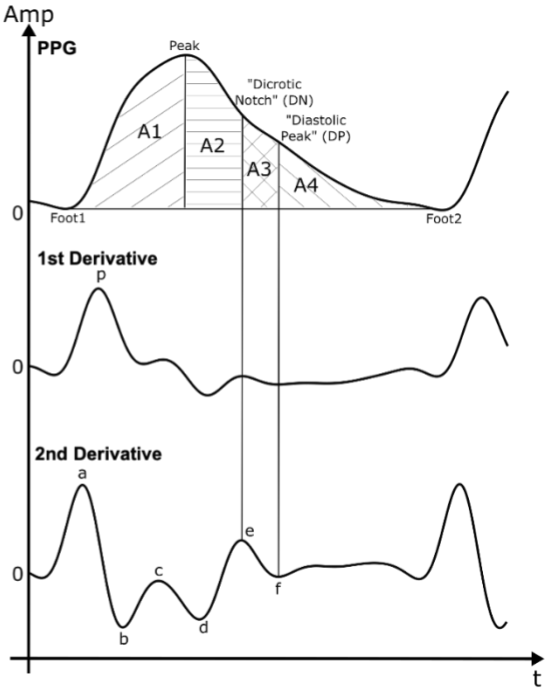

Figure 15: 31 PPG waveform features considered. A total of 31 popular or promising PPG waveform features [80], [81] were considered as candidates for predicting the intervention-induced BP changes. Subject demographic information and pulse arrival time (PAT, the time delay between the R-wave of the ECG waveform and the leading foot of the PPG waveform) were also possible features. While other features were also commonly used in literature, many of them were not well-defined and did not always exist, even in a PPG waveform of high signal quality. We used the features that were able to be well-defined.

Model Development

We sought to develop linear regression models to predict the BP changes relative to the first or "baseline" cuff BP measurement of each subject. We thus subtracted the baseline cuff BP/waveform feature value from the remaining cuff BP/waveform features values of each subject. We also normalized each waveform feature change with the baseline feature value (unless it was near zero). In addition, we allowed age, gender (1 or 2), height, weight, and the baseline cuff BP values as possible person features. The models for mapping waveform features (w) and person features (p) to BP (P_x with $x = s$ for systolic and $x = d$ for diastolic) via linear parameters (α) thus took on the following form:

$$P_x^{i,j} - P_x^{1,j} = \sum_{k=1}^{m} \alpha_k \left(\frac{w_k^{i,j} - w_k^{1,j}}{w_k^{1,j}} \quad \text{or} \quad p_k^j \right) + e_x^{i,j},$$

where the superscripts i and j denote ith value of the jth subject; the subscript k signifies the kth feature; m indicates the number of features (model order); and e is the model residual error. For gender, we used two features to effectively define one model intercept for males and another model intercept for females.

We selected the features and estimated the model parameters and order using forward stepwise regression with an "elbow" method. We added one feature at a time to the model, starting with zero features and ending with six features, and selected the new feature at each iteration as the one that minimized the mean square of the residual error. We conservatively chose six as the maximal model order, as 20-30 data points are typically needed to estimate one parameter and about 180 data points were available to estimate the BP change prediction model. In post hoc analysis, the results proved to be insensitive to small changes to the maximal model order. We then fitted two lines to the monotonically decreasing curve relating mean squared residual error to the model order and selected the order, and thus the final model, via the intersection of the two lines. We found that this empirical method to identify the curve elbow yielded more parsimonious models than other methods such as lasso and ridge regression.

We employed the above steps in a leave-one-out cross validation framework. We specifically estimated 32 models using data from all combinations of 31 of the subjects and left the remaining subject data for testing each model. In this way, we leveraged as much data as possible for training while also allowing testing on all subjects without using the same data for training and testing. We created separate models for the finger, toe, and ear PPG waveforms to predict the different changes in SP and DP and thus arrived at six PPG waveform feature models.

For comparison, we also created three reference models. The first model is to use the baseline cuff BP value as the predictor of the ensuing BP (i.e., no BP changes) in the subject ("baseline BP reference model"). The second model is to predict the BP changes from the person features using the stepwise regression, elbow, and leave-one-out methods ("demographic reference model"). The third model is to predict the BP changes from only 1/PAT, which correlated slightly better than PAT to BP here, for each PPG waveform using regression and leave-one-out methods ("PAT reference model").

Model Evaluation

We evaluated the 182 pooled BP change predictions of each model against the reference cuff measurements from the 32 leave-one-out test subjects using standard correlation and Bland-Altman analyses. We computed the Bland-Altman bias and precision errors (μ and σ) via the basic sample mean and SD of the errors, as mixed effects modeling to account for the repeated measures per subject [82] hardly impacted the σ. To conveniently quantify the overall error, we used the RMSE = $\sqrt{(\mu^2+\sigma^2)}$.

We used the RMSE metric to perform statistical comparisons of two models (i.e., PPG waveform feature model versus a reference model). We applied non-parametric cluster bootstrapping to calculate confidence intervals and make the comparisons [83]. We took 10,000 random samples of the 32 subjects with replacement of the subjects. The number of subjects in each sample was 32, and we included all BP change errors from a subject per sample. For each sample, we computed the RMSE as described above for each model and the difference between the RMSEs of the two models for comparison (model 1 – model 2). We calculated both 95% CIs

of each RMSE and of each RMSE difference from the corresponding distribution of 10,000 values via a standard percentile bootstrap.

Table 4: Root-mean-squared-errors (RMSEs) of the intervention-induced blood pressure (BP) changes predicted by the models against the reference cuff BP measurements

Models	RMSE (lower and upper 95% CIs) (Mean (μ) ± SD (σ))	
	SP (Systolic BP)	DP (Diastolic BP)
Baseline BP Reference	**10.9 (9.5 - 12.4) (3.7 ± 10.2)**	**6.5 (5.6 - 7.3) (0.9 ± 6.4)**
Demographic Reference	**10.8 (9.2 - 12.7) (0.5 ± 10.8)**	**6.6 (5.7 - 7.5) (0.0 ± 6.6)**
Finger PAT Reference	**10.1 (8.6 - 11.8) (2.8 ± 9.7)**	**6.3 (5.5 - 7.1) (0.6 ± 6.3)**
Ear PAT Reference	**10.2 (8.6 - 11.9) (1.7 ± 10.1)**	**6.5 (5.6 - 7.4) (0.6 ± 6.5)**
Toe PAT Reference	**9.1 (7.6 - 10.9) (2.1 ± 8.9)**	**6.2 (5.3 - 7.1) (0.4 ± 6.2)**
Finger PPG Waveform Feature $SP^i = 80.6\left(\frac{1}{PAT}\right)^i + 50.4\left(b\text{-}time^i\right)_+ SP^1$	**9.5 (7.9 - 11.5)*† (2.3 ± 9.3)**	**7.0 (6.1 - 7.7) (0.5 ± 7.0)**
Ear PPG Waveform Feature $SP^i = 30.2\left(\frac{1}{PAT}\right)^i + 26.2\left(STT^i\right)_+ SP^1$ $DP^i = 30.6\left(STT^i\right) - 40.4\left(PW^i\right)_+ DP^1$	**9.5 (7.8 - 11.4)*† (0.7 ± 9.5)**	**5.7 (5.0 - 6.3)* (0.2 ± 5.7)**
Toe PPG Waveform Feature $SP^i = 141.9\left(\frac{1}{PAT}\right)^i + SP^1$	**9.1 (7.6 - 10.9)* (2.1 ± 8.9)**	**6.5 (5.6 - 7.4) (0.2 ± 6.5)**

*denotes statistical significance ($p < 0.05$ with Holm's correction for multiple comparison) versus baseline BP reference model (which predicts BP during the interventions simply via the baseline cuff BP measurement) and † denotes statistical significance versus corresponding pulse arrival time (PAT) reference model (which predicts the BP changes via 1/PAT alone). The demographic reference model (which predicts the BP changes via subject age, height, weight, gender, and baseline cuff BP) did not offer value and was not compared. The PPG waveform feature models are shown only if they provided added value. Each feature (1/PAT, b-time, STT, and PW as defined in Fig. 14) actually represents the current feature minus the baseline feature divided by the baseline feature as shown in Fig. 15.

If the upper CI for the RMSE difference were less than zero, then model 1 would be considered superior to model 2. Since we made six comparisons, we applied a Holm's correction [84] such that a two-sided $p < 0.05/(6+1-k)$, where k is the comparison with the kth lowest p-value (i.e., X = 99.17 for k = 1), was considered statistically significant.

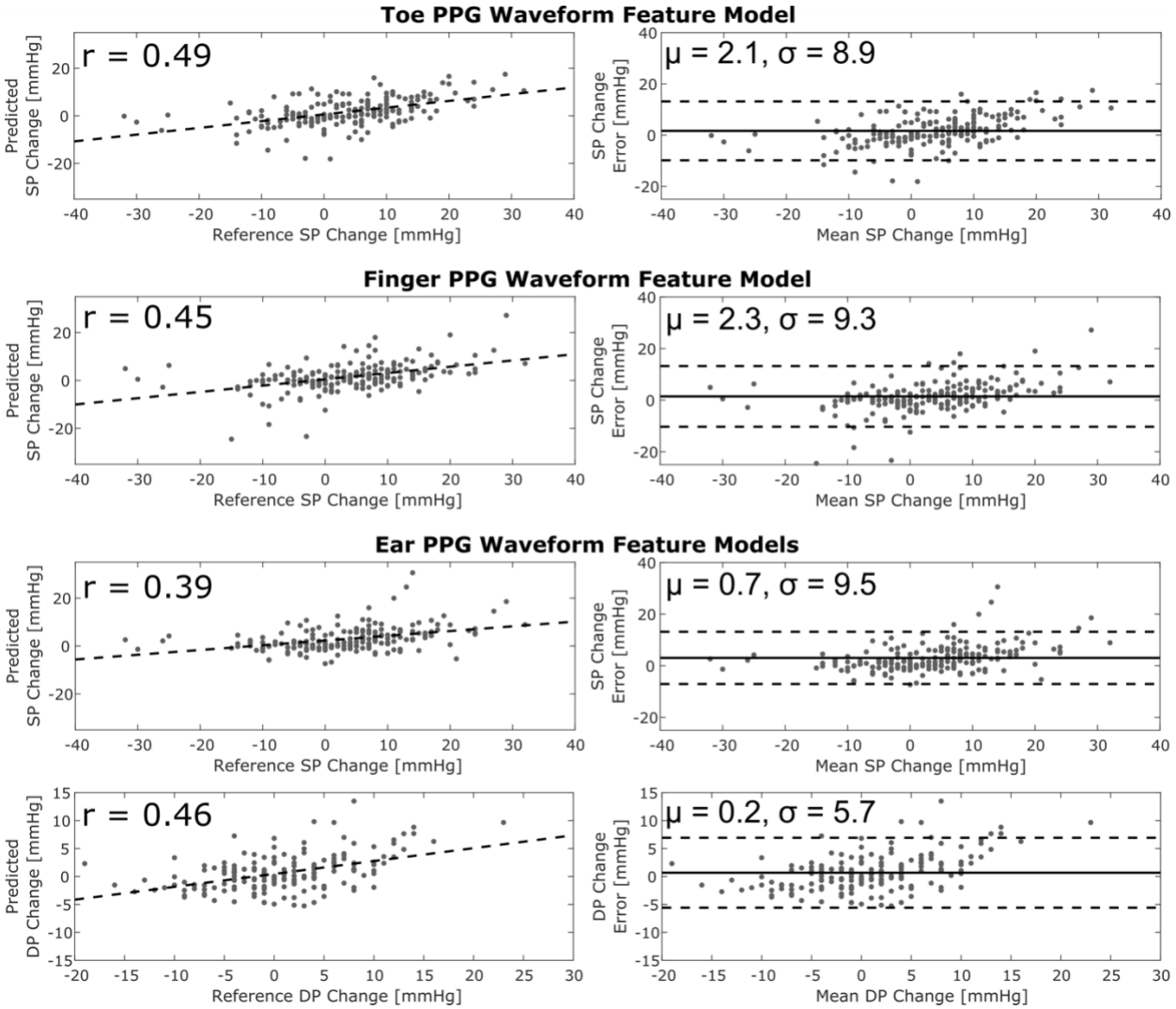

Figure 16: Correlation and Bland-Altman plots of estimated and reference BP. Correlation and Bland-Altman plots of BP changes predicted by the PPG waveform feature models that offered added value versus the reference cuff BP measurements. M = 182 measurements from N = 32 subjects. The dashed line in the correlation plots is the best-fit line; r is the correlation coefficient; and μ and σ are bias and precision errors respectively in mmHg. While the toe PPG waveform feature model shows most correlation with the reference cuff BP, the ear PPG waveform PPG model produced a more significant improvement from the baseline BP reference.

Results

A total of 214 PPG-BP measurement sets from 32 subjects (50% female; 52 (17) (mean (SD)) years of age; 166 (10) cm in height; 89 (34) kg in weight; 25% with treated hypertension; 31% with smoking history; and 9% with LDL cholesterol >=190 mg/dL) formed the study data. The baseline SP and DP (mean± standard error (SE)) were 121±3 and 79±2 mmHg (N=32). Table 4 shows the results of the PPG waveform feature models versus reference models in leave-one-out prediction of the intervention-induced BP changes relative to the subject baseline values (M=182). This table also presents those models that proved to be useful. Each of the useful models was stable across the 32 leave-one out training sets in the sense that 97-100% of the 32 models yielded the same features, and the models displayed in the table are representative ones resulting from training on all 32 subject datasets.

The baseline BP reference model, which simply employs the baseline cuff BP of each subject to predict the ensuing BP, yielded RMSEs of 10.9 mmHg for SP and 6.5 mmHg for DP. While these error levels are near or within the regulatory limits of 5 and 8 mmHg bias and precision errors [63], the BP change prediction models must yield lower errors to offer any value. The demographic reference model, which includes subject age, gender, height, weight, and the baseline cuff SP and DP as candidate features, provided no such value. The PAT reference models, which include the time delay as the sole feature, were helpful in predicting changes in SP but not DP. As shown previously [68], toe PAT was clearly the best in tracking the SP changes.

Three of the six PPG waveform feature models afforded added value over the reference models. The finger and ear PPG waveform feature models for predicting SP changes included 1/PAT as the primary feature and the b-time (time to the minimum second derivative of the PPG waveform) or STT (amplitude divided by the maximum derivative of the PPG waveform) as a

secondary feature, all with positive regression parameters. These models yielded RMSEs of 9.5 mmHg ($p < 0.022$ versus baseline BP and finger and ear PAT reference models). The ear PPG waveform feature model for predicting DP changes included STT as the primary feature with positive regression parameter and PW (pulse width) as a secondary feature with negative regression parameter. This model produced an RMSE of 5.7 mmHg ($p = 0.003$ versus baseline BP reference model). Note that the toe PPG waveform feature model for predicting SP changes included only 1/PAT as input. However, this model yielded an RMSE of 9.1 mmHg ($p = 0.004$ versus baseline BP reference model).

Fig. 16 shows correlation and Bland-Altman plots of the BP change predictions of the four useful PPG waveform feature models versus the reference cuff BP measurements (M=182). These results allow visualization of the key numerical results in the Table and also indicate that the correlation coefficients between the predicted and reference BP changes were 0.39-0.49.

In sum, the b-time and STT, which are time intervals of the fast upstroke, of ear and finger but not toe PPG waveforms were the only useful features in tracking changes in BP. For SP, these PPG fast upstroke time intervals were helpful in conjunction with PAT but not as standalone features. For DP, STT of the ear PPG waveform was useful by itself. The PPG fast upstroke time intervals were positively rather than negatively related to the BP changes. They reduced the BP change RMSEs of the reference models by 6-13%.

Discussion

PPG waveform analysis is being increasingly investigated for ultra-convenient BP monitoring [69]–[75]. However, this data-driven approach is not well understood in terms of both efficacy and useful features and models. In this study, we sought to develop easy-to-understand

models relating PPG waveform features to BP changes (after a single cuff calibration) and to determine conclusively whether they provide added value or not in BP measurement accuracy.

We analyzed finger, toe, and ear PPG waveforms along with ECG waveforms and reference manual cuff BP measurements from 32 normotensive and hypertensive volunteers during a battery of challenging interventions that changed SP and DP differently (see Figs. 13 and 14). These data thus allowed us to create six PPG waveform feature models for predicting intervention-induced BP changes corresponding to the three PPG waveforms and two BP levels.

PPG Waveform Feature Models:

Finger:

$$SP^i = 80.6\left(\frac{\left(\frac{1}{PAT}\right)^i-\left(\frac{1}{PAT}\right)^1}{\left(\frac{1}{PAT}\right)^1}\right) + 50.4\left(\frac{\text{b-time}^i-\text{b-time}^1}{\text{b-time}^1}\right)+ SP^1$$

Ear:

$$SP^i = 30.2\left(\frac{\left(\frac{1}{PAT}\right)^i-\left(\frac{1}{PAT}\right)^1}{\left(\frac{1}{PAT}\right)^1}\right) + 26.2\left(\frac{STT^i-STT^1}{STT^1}\right) + SP^1$$

$$DP^i = 30.6\left(\frac{STT^i-STT^1}{STT^1}\right) - 40.4\left(\frac{PW^i-PW^1}{PW^1}\right) + DP^1$$

Toe:

$$SP^i = 141.9\left(\frac{\left(\frac{1}{PAT}\right)^i-\left(\frac{1}{PAT}\right)^1}{\left(\frac{1}{PAT}\right)^1}\right) + SP^1$$

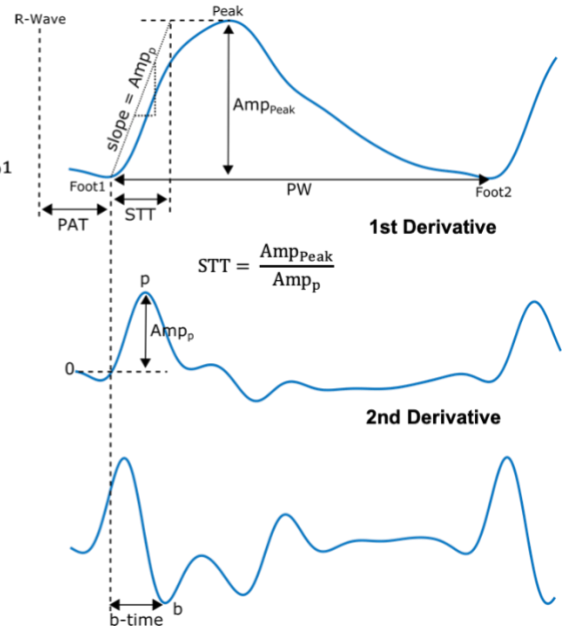

Figure 17: The PPG waveform feature models that were useful in predicting BP changes. The b-time and STT, which are PPG fast upstroke time intervals (see Fig. 15 for definitions), reduced the BP change RMSE relative to reference models not including PPG waveform features as input by about 10% (see Table 4). The superscript i is the i^{th} measurement; i=1, baseline measurement for cuff calibration.

We chose analysis tools to create models that are readily interpretable and effective when the subject number is not high. More specifically, we limited the candidate features to popular or promising PPG waveform features (see Fig. 15) plus subject demographic information and PAT (time delay between ECG R-wave and PPG foot); applied stepwise linear regression for forward selection of the features and estimation of the model parameters; used a parsimonious elbow

method for determining the number of features; and employed leave-one-out cross validation to leverage the data as much as possible for independent training and testing. We also verified our approach in terms of robustness to user-selected variables and overfitting relative to other tools.

We assessed the BP changes relative to the subject baseline BP predicted by the PPG waveform feature models against the reference cuff BP measurements using standard Bland-Altman and correlation analysis. Crucially, to ascertain added value, we compared the BP change RMSEs of these models to reference models without PPG waveform features as input (e.g., demographic or PAT models). We performed these comparisons statistically via cluster bootstrapping while reducing the significance level for multiple comparisons.

Fig. 17 presents the four PPG waveform feature models that showed added value in predicting BP changes. Note that the toe PPG waveform feature model included only PAT as input. The other three models each included a PPG waveform feature and reduced the RMSE of the reference models by about 10% (see Table 4). The correlations between the predicted BP changes of the four models and the reference measurements were about 0.4-0.5 (see Fig. 16).

Hence, almost all of the 31 candidate features for study were of no value in tracking the BP changes despite their popularity [80]. In fact, a number of these features were often not well defined (e.g., t_c, t_d, t_e, t_f, Amp_{DN}, and Amp_{DP}) and thus suffered from substantial variability, which surely reduced their utility. This limitation of the considered features has been noted before [80], [85]. Only the b-time (t_b) and STT, which were generally well defined and reflect the fast upstroke time interval of the PPG waveform, showed value in BP measurement.

However, the PPG fast upstroke time intervals were positively related to the BP changes. This finding opposes conventional thinking that an increase in cardiac contractility or preload (via, e.g., exercise) would increase BP while reducing the PPG upstroke interval to create a negative

relationship. STT was also introduced as a single-site measurement of PTT and shown to be positively related to PTT and thus inversely related to BP [81]. The positive relationship that we found may be due to small artery viscoelasticity. As we previously found [86], as BP increases, the cutoff frequency of the viscoelastic lowpass filter may decrease such that the PPG upstroke time interval increases (see Equation in Introduction). This viscoelastic mechanism could be most important over a range of BP interventions, especially for fast upstroke time intervals in which the lowpass filtering effect would be more pronounced. Note that, even if the PPG fast upstroke time interval decreases during exercise, the models in Fig. 17 may still correctly predict BP increases via the other feature in these models.

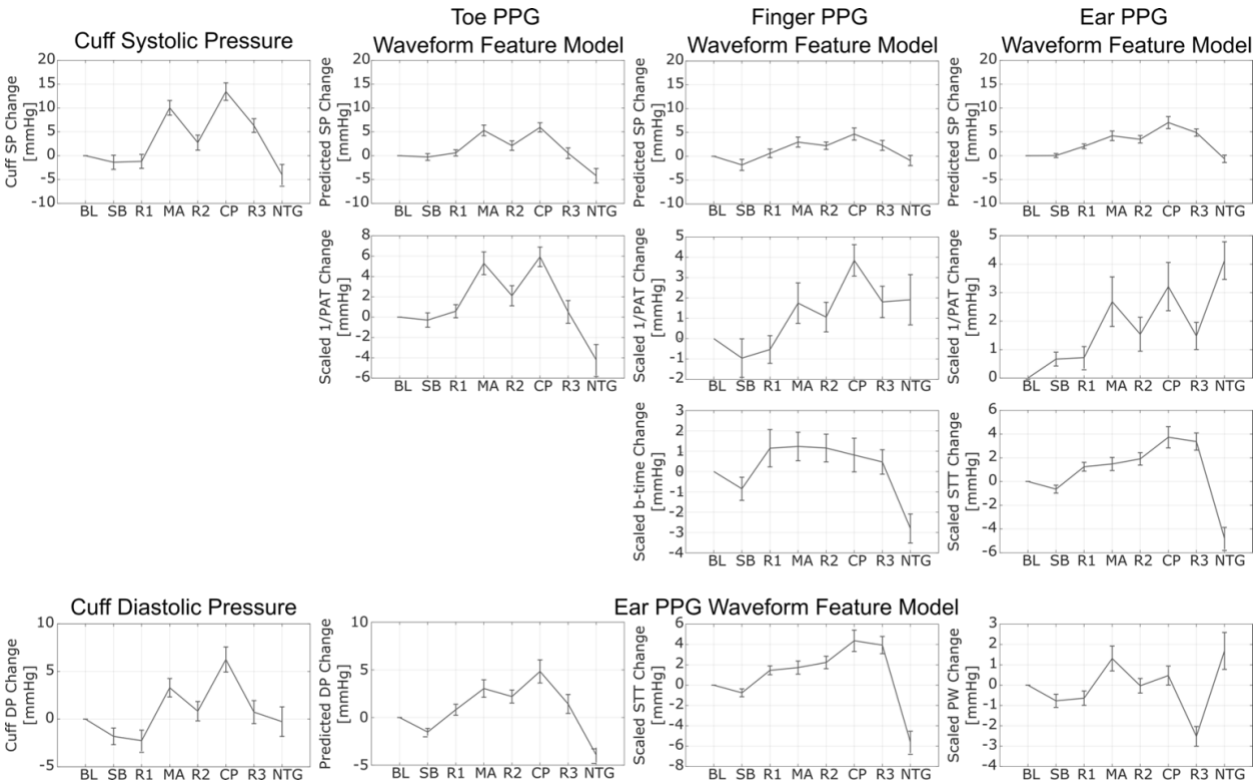

Figure 18: Subject average trends of reference cuff BP changes and predicted BP changes with the models shown in Fig. 17 over the interventions shown in Fig. 14. Each feature in each model is also shown after scaling by its model parameter to yield the component of BP in units of mmHg predicted by that feature. These trends help explain how the PPG fast upstroke time intervals add value to BP measurement accuracy. Values are mean±SE.

In fact, a PPG fast upstroke time interval was only of added value in predicting changes in SP when combined with PAT. Fig. 18 shows the subject average trends of the reference SP and DP changes and of each feature, scaled by its associated model parameter, of each of the four models over the interventions. The so-calibrated finger and ear 1/PAT trends appear to track the SP trend well except for the nitroglycerin (NTG) intervention, and the calibrated PPG fast upstroke time interval seems to be of most value for this intervention without significantly compromising the other interventions. The steep decline in the PPG fast upstroke time interval after NTG may be due to the reduction in SP as well as smooth muscle relaxation, which could both conceivably increase the viscoelastic lowpass filter cutoff frequency. However, PPG waveform features alone did add value in predicting changes in DP. The calibrated PW (pulse width) appears to help STT in tracking of the DP trend during a few interventions including mental arithmetic (MA) and NTG, which both increased the heart rate. For SP or DP, Fig. 18 shows that STT, which again stands for "slope transit time", is not negatively related to BP in general and may thus benefit from a name change.

However, the PPG fast upstroke time interval is not always of added value and the precise definition matters. Fig. 19 illustrates typical toe, ear, and finger PPG waveform beats over a segment and their first and second derivatives. The toe PPG waveform tended to be noisier than the other two PPG waveforms, so the fast upstroke time intervals were more variable and thus not selected for the toe PPG waveform feature model. The ear PPG waveform tended to have a wider peak region such that the b-time was more variable than STT, and the latter feature was selected for the ear PPG waveform feature model. Both the b-time and STT were relatively consistent for the finger PPG waveform, but the b-time happened to provide more value. Hence, PPG waveform analysis for tracking BP changes depends importantly on the measurement site. While back-of-

the-wrist PPG waveforms are popular due to their convenience in watch form factors [75], these waveforms are notoriously poor in quality. It is thus difficult to imagine that they could have yielded more or as useful features for tracking BP changes in this study.

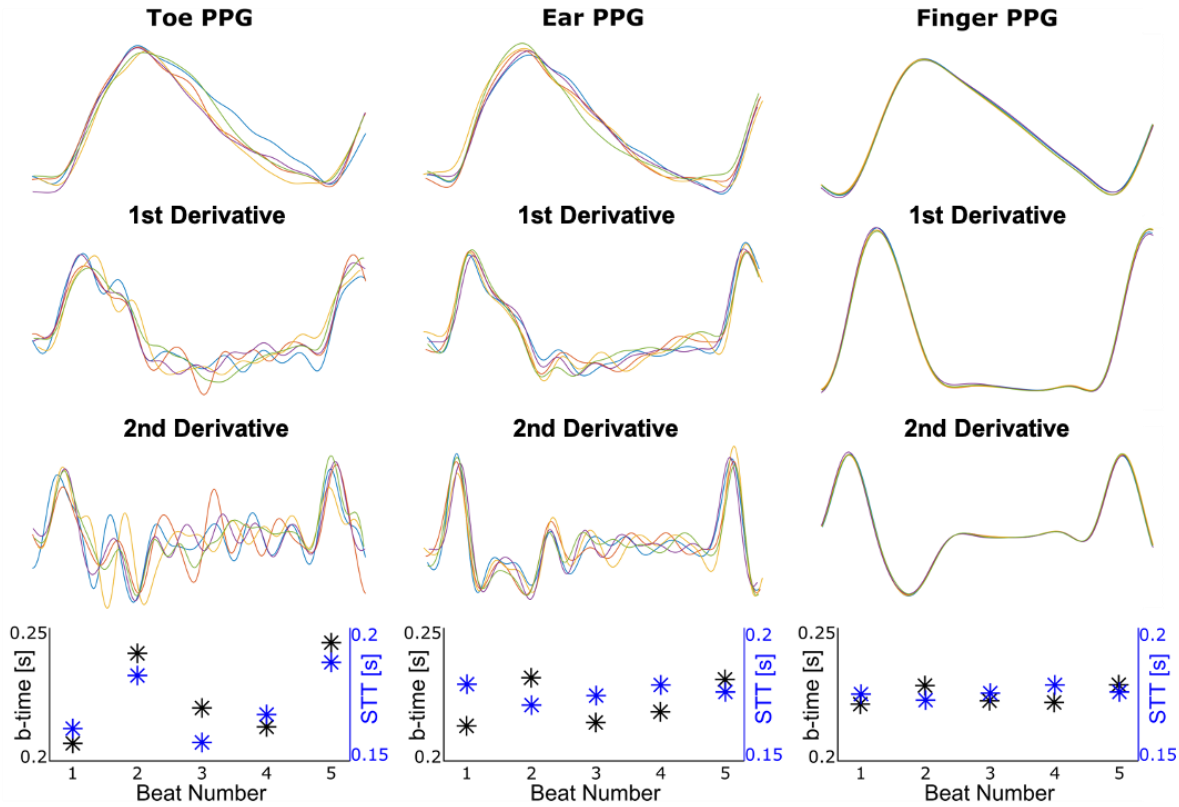

Figure 19: Example of toe, ear, and finger PPG waveform beats from an intervention indicating the typical extent of variability of the fast upstroke time intervals. This example helps explain why measurement site and precise definition of the fast upstroke time interval made a difference.

In this laboratory investigation, the PPG sensor contact pressure (the external pressure applied by the sensor on the skin) was likely maintained throughout the BP changes. However, in practice, PPG sensor contact pressure can vary with, for example, replacement of a fingertip on a smartphone PPG sensor for on-demand measurement or putting a smartwatch with PPG sensor on the wrist each day for continuous measurement. We previously showed that the maximum change in finger PAT over a physiologic range of finger PPG sensor contact pressures (30-80 mmHg) was

22±2 ms despite no change in BP in 17 healthy subjects [86]. We applied the finger PPG waveform feature model in Fig. 17 to the same data here to gain some quantitative understanding of the impact of PPG sensor contact pressure variations on PPG waveform analysis for BP measurement. We found that the maximum change in SP predicted by the finger PPG waveform feature model over the physiologic contact pressure range was 12.0±1.7 mmHg. For comparison, the maximum predicted SP change of the finger PAT reference model found in this study (see Table 4) was 7.2±0.7 mmHg. Hence, as expected, PPG waveform analysis is significantly more impacted by PPG sensor contact pressure variations than PAT (67% here). Since the regulatory bias and precision error limits are again 5 and 8 mmHg [63], these additional findings underscore the importance of controlling for PPG sensor contact pressure when applying PPG waveform analysis for BP tracking in practice.

A strength of this study is the use of challenging interventions to change BP in subjects relevant to hypertension applications. At the same time, these interventions, especially NTG, are not simple to employ and limited the number of subjects for study. As a result, we had to confine our analysis tools and could not explore more exhaustive candidate feature sets and nonlinear models. Including more features and nonlinear combinations of features would result in overfitting here and thus false alarms in the selected features. While we also could not investigate calibration-free prediction of BP from PPG waveforms, this approach is far less viable based on first principles. Another limitation of this study is that we did not record the DC component of the PPG waveforms. Normalizing the AC component by the DC component could improve the value of features involving the PPG amplitude (but not PPG time intervals) by mitigating the variability in environmental conditions (which were largely controlled in this study) or skin pigmentation.

However, such normalization would likely not have helped improve the PPG peak-to-peak amplitude in tracking the BP changes here (see Fig. 13).

In conclusion, we have explicitly presented readily interpretable models to relate PPG waveform features to BP changes in human subjects and have clearly shown that they can afford some added value in BP measurement accuracy. Future investigations should test the generalizability of these models, especially the PPG fast upstroke intervals therein, as well as create extensive and relevant training datasets to more fully explore the value of PPG waveform analysis in cuff-less BP measurement.

CONCLUSION

Current oscillometric devices for monitoring central BP maintain the cuff pressure at a constant level to acquire a pulse volume plethysmography (PVP) waveform and calibrate it to brachial BP levels estimated with population average methods. A physiologic method was developed to further advance central BP measurement. A patient-specific method is applied to estimate brachial BP levels from a cuff pressure waveform obtained during conventional deflation via a nonlinear arterial compliance model. A physiologic method is then employed to extract the PVP waveform from the same waveform via ensemble averaging and calibrate it to the brachial BP levels. A method based on a wave reflection model is thereafter employed to define a variable transfer function, which is applied to the calibrated waveform to derive central BP. This method was evaluated against invasive central BP measurements from patients. The method yielded central SP, DP, and PP bias and precision errors of -0.6 to 2.6 and 6.8 to 9.0 mmHg. The conventional oscillometric method produced similar bias errors but precision errors of 8.2 to 12.5 mmHg ($p \leq 0.01$). The new method can derive central BP more reliably than some current non-invasive devices and in the same way as traditional cuff BP.

We developed an iPhone X application to measure BP via the "oscillometric finger pressing method". The user presses her fingertip on both the front camera and screen to increase the external pressure of the underlying artery, while the application measures the resulting variable-amplitude blood volume oscillations via the camera and applied pressure via the strain gauge array under the screen. The application also visually guides the fingertip placement and actuation and then computes BP from the measurements just like many automatic cuff devices. We tested the application, along with a finger cuff device, against a standard cuff device. The application yielded

bias and precision errors of -4.0 and 11.4 mmHg for SP and -9.4 and 9.7 mmHg for DP (n = 18). These errors were near the finger cuff device errors. This proof-of-concept study surprisingly indicates that cuff-less and calibration-free BP monitoring may be feasible with many existing and forthcoming smartphones.

Finally, we developed easy-to-understand models relating PPG waveform features to BP changes (after a single cuff calibration) and determined conclusively whether they provide added value or not in BP measurement accuracy. Stepwise linear regression was employed so as to create parsimonious models for predicting the intervention-induced BP changes from popular PPG waveform features, pulse arrival time (PAT, time delay between ECG R-wave and PPG foot), and subject demographics. The finger b-time (PPG foot to minimum second derivative time) and ear STT (PPG amplitude divided by maximum derivative), when combined with PAT, reduced the systolic BP change prediction RMSE of reference models by 6-7% ($p<0.022$). The ear STT together with the pulse width reduced the diastolic BP change prediction RMSE of the reference model by 13% ($p=0.003$). Hence, PPG fast upstroke time intervals can offer some added value in cuff-less measurement of BP changes.

A strength of this study is the use of challenging interventions to change BP in subjects relevant to hypertension applications. At the same time, these interventions, especially NTG, are not simple to employ and limited the number of subjects for study. As a result, we had to confine our analysis tools and could not explore more exhaustive candidate feature sets and nonlinear models. Including more features and nonlinear combinations of features would result in overfitting here and thus false alarms in the selected features. While we also could not investigate calibration-free prediction of BP from PPG waveforms, this approach is far less viable based on first principles. Another limitation of this study is that we did not record the DC component of the PPG

waveforms. Normalizing the AC component by the DC component could improve the value of features involving the PPG amplitude (but not PPG time intervals) by mitigating the variability in environmental conditions (which were largely controlled in this study) or skin pigmentation. However, such normalization would likely not have helped improve the PPG peak-to-peak amplitude in tracking the BP changes here (see Fig. 13).

In conclusion, we have explicitly presented readily interpretable models to relate PPG waveform features to BP changes in human subjects and have clearly shown that they can afford some added value in BP measurement accuracy.

FUTURE WORK

We introduced a physiologic method to both mitigate the calibration error and obtain central BP measurements in the exact same way as traditional automatic cuff BP measurements. We showed that this method can yield central BP measurements that agree with gold standard reference measurements to a significantly greater degree than some current non-invasive devices. Future investigations may be worthwhile to confirm the accuracy of the new method, especially in a real-time device, and apply it broadly to determine the full clinical potential of central BP.

The iPhone application errors are close to our previous device [30]. However, the application did not yield BP in two users due to finger pressing contact area mis-estimation, which is not a factor for the device. The application also yielded more try-again messages (about 50 versus 40%) and less repeatable BP measurements (e.g., mean absolute difference between successive measurements at heart level of about 7 versus 5 mmHg) likely due to variability in fingertip positioning despite the rectangular box guide. Hence, not surprisingly, the application may be less effective than our device, which employs application-specific sensors.

However, any reduction in effectiveness may be offset by the increased accessibility of a smartphone application. An estimated 50 million iPhone X models have already been sold [60]. Moreover, other smartphones have 3D Touch capability including iPhone models 6S and higher [56] and the Huawei Mate S model [61]. Hence, applications for these phones may likewise be developed (with appropriate modifications for differing arrangements of the camera/PPG sensor and screen). In 2017, 328 million iPhones with 3D Touch capability (excluding iPhone 8 and X) were being used [62]. Hence, it is conceivable that the oscillometric finger pressing method could reach about 500 million smartphones already in use.

Our iPhone application should be improved. Most importantly, the finger pressing contact area was mis-estimated in two subjects and variably estimated in some other subjects due to fingertip mis-positioning. In practice, when the application consistently outputs try-again messages or unusual BP measurements, the area could be determined with just one cuff BP measurement (as opposed to periodic cuff calibrations required by competing methods [16], [55]). The application could also output a running average of the past several BP measurements (instead of individual BP measurements) to mitigate random variability resulting from fingertip mis-positioning and other factors [55]. In this way, the application may be able to yield BP errors that are closer to the putative bias and precision errors limits of 5 and 8 mmHg [63] than the results reported herein. However, there may be better solutions. One possibility is to measure the area (even at different finger pressures) via the fingerprint sensor under the screen for authentication in upcoming smartphones including the 2019 iPhone X [64]. The optimal solution is if Apple were to provide access to an accurate area measurement as the user performs the actuation via the capacitive sensor array also under the screen [56]. Such access may be possible, as superior area assessment may be obtained with Android devices [65]. In addition, the infrared camera also on the notch of the iPhone X (Fig. 10a) for authentication may be used to provide higher-fidelity blood volume oscillations in cold and other low signal conditions [66]. Finally, the BP computation algorithm needs further development to satisfy the accuracy requirements of a regulatory test [63]. In summary, this proof-of-concept study surprisingly indicates that cuff-less and calibration-free BP monitoring may be feasible with many existing and forthcoming smartphones by leveraging sensors built-in for other purposes. Such ubiquitous BP monitoring may improve hypertension awareness and control rates and thereby help reduce the incidence of cardiovascular disease and mortality.

We have explicitly presented readily interpretable models to relate PPG waveform features to BP changes in human subjects and have clearly shown that they can afford some added value in BP measurement accuracy. Future investigations should test the generalizability of these models, especially the PPG fast upstroke intervals therein, as well as create extensive and relevant training datasets to more fully explore the value of PPG waveform analysis in cuff-less BP measurement.

BIBLIOGRAPHY

BIBLIOGRAPHY

[1] E. J. Benjamin *et al.*, "Heart disease and stroke statistics-2019 update: A report from the American Heart Association," *Circulation*, vol. 139, no. 10, pp. e56–e528, Mar. 2019, doi: 10.1161/CIR.0000000000000659.

[2] D. S. Picone *et al.*, "Accuracy of cuff-measured blood pressure," *J. Am. Coll. Cardiol.*, vol. 70, no. 5, pp. 572–586, Aug. 2017, doi: 10.1016/j.jacc.2017.05.064.

[3] A. Chockalingam, "Impact of world hypertension day," *Can. J. Cardiol.*, vol. 23, no. 7, pp. 517–519, 2007.

[4] B. M. Psaty *et al.*, "Health outcomes associated with antihypertensive therapies used as first-line agents : A systematic review and meta-analysis," *JAMA J. Am. Med. Assoc.*, vol. 277, no. 9, pp. 739–745, 1997, doi: 10.1001/jama.1997.03540330061036.

[5] M. M. Ibrahim and A. Damasceno, "Hypertension in developing countries," *Lancet*, vol. 380, no. 9841, pp. 611–619, 2012, doi: 10.1016/S0140-6736(12)60861-7.

[6] "Heart failure projected to increase dramatically, according to new statistics," *American Heart Association News*, 2017. https://news.heart.org/heart-failure-projected-to-increase-dramatically-according-to-new-statistics/ (accessed Sep. 06, 2018).

[7] T. G. Pickering, D. Shimbo, and D. Haas, "Ambulatory blood-pressure monitoring," *N. Engl. J. Med.*, vol. 354, no. 22, pp. 2368–2374, 2006, doi: 10.1056/NEJMra060433.

[8] R. Agarwal, J. E. Bills, T. J. W. Hecht, and R. P. Light, "Role of home blood pressure monitoring in overcoming therapeutic inertia and improving hypertension control: a systematic review and meta-analysis," *Hypertension*, vol. 57, no. 1, pp. 29–38, 2011, doi: 10.1161/HYPERTENSIONAHA.110.160911.

[9] D. Perloff *et al.*, "Human blood pressure determination by sphygmomanometry," *Circulation*, vol. 88, no. 5 Pt 1, pp. 2460–2470, 1993.

[10] B. S. Alpert, D. Quinn, and D. Gallick, "Oscillometric blood pressure: a review for clinicians," *J. Am. Soc. Hypertens.*, vol. 8, no. 12, pp. 930–938, 2014, doi: 10.1016/j.jash.2014.08.014.

[11] G. M. Drzewiecki, R. Hood, and H. Apple, "Theory of the oscillometric maximum and the systolic and diastolic detection ratios," *Ann. Biomed. Eng.*, vol. 22, no. 1, pp. 88–96, 1994.

[12] G. A. van Montfrans, "Oscillometric blood pressure measurement: progress and problems," *Blood Press. Monit.*, vol. 6, no. 6, pp. 287–290, 2001.

[13] L. A. Geddes, M. Voelz, C. Combs, D. Reiner, and C. F. Babbs, “Characterization of the oscillometric method for measuring indirect blood pressure,” *Ann. Biomed. Eng.*, vol. 10, no. 6, pp. 271–280, 1982, doi: 10.1007/BF02367308.

[14] B. P. Imholz, W. Wieling, G. A. van Montfrans, and K. H. Wesseling, “Fifteen years experience with finger arterial pressure monitoring: assessment of the technology,” *Cardiovasc. Res.*, vol. 38, no. 3, pp. 605–616, 1998.

[15] K. Wesseling, B. Wit, and G. Hoeven, “Physiocal, calibrating finger vascular physiology for Finapres,” *Homeostasis*, vol. 36, no. 2–3, pp. 67–82, 1995.

[16] R. Mukkamala *et al.*, “Toward ubiquitous blood pressure monitoring via pulse transit time: Theory and practice,” *IEEE Trans. Biomed. Eng.*, vol. 62, no. 8, pp. 1879–1901, Aug. 2015, doi: 10.1109/TBME.2015.2441951.

[17] P. Gizdulich, A. Prentza, and K. Wesseling, “Models of brachial to finger pulse wave distortion and pressure decrement,” *Cardiovasc. Res.*, vol. 33, no. 3, pp. 698–705, Mar. 1997, doi: 10.1016/S0008-6363(97)00003-5.

[18] J. S. Eckerle, “Tonometry, arterial,” in *Encyclopedia of Medical Devices and Instrumentation*, J. G. Webster, Ed. New York, NY, USA: Wiley, 1988.

[19] G. L. Pressman and P. M. Newgard, “A transducer for the continuous external measurement of arterial blood pressure,” *IEEE Trans. Bio-Medical Electron.*, vol. 10, no. 2, pp. 73–81, 1963, doi: 10.1109/TBMEL.1963.4322794.

[20] S. Hansen and M. Staber, “Oscillometric blood pressure measurement used for calibration of the arterial tonometry method contributes significantly to error,” *Eur. J. Anaesthesiol.*, vol. 23, no. 9, pp. 781–787, 2006, doi: 10.1017/S0265021506000688.

[21] “National High Blood Pressure Education Program (NHBPEP)/National Heart, Lung, and Blood Institute (NHLBI) and American Heart Association (AHA) Working meeting on blood pressure measurement,” 2002. https://www.nhlbi.nih.gov/files/docs/resources/heart/bpmeasu.pdf (accessed Dec. 22, 2019).

[22] J. Liu *et al.*, “Patient-specific oscillometric blood pressure measurement,” *IEEE Trans. Biomed. Eng.*, vol. 63, no. 6, pp. 1220–1228, 2016, doi: 10.1109/TBME.2015.2491270.

[23] J. Liu, H.-M. Cheng, C.-H. Chen, S.-H. Sung, J.-O. Hahn, and R. Mukkamala, “Patient-specific oscillometric blood pressure measurement: Validation for accuracy and repeatability,” *IEEE J. Transl. Eng. Heal. Med.*, vol. 5, no. 1900110, p. 1900110, Dec. 2016, doi: 10.1109/JTEHM.2016.2639481.

[24] W. W. Nichols, M. F. O’Rourke, and C. Vlachopoulos, *McDonald’s blood flow in arteries; theoretical, experimental and clinical principles*, vol. 23, no. 1. CRC Press,

1992.

[25] C. Vlachopoulos, K. Aznaouridis, M. F. O'Rourke, M. E. Safar, K. Baou, and C. Stefanadis, "Prediction of cardiovascular events and all-cause mortality with central haemodynamics: a systematic review and meta-analysis," *Eur. Heart J.*, vol. 31, no. 15, pp. 1865–1871, 2010.

[26] K. Natarajan *et al.*, "Central blood pressure monitoring via a standard automatic arm cuff," *Sci. Rep.*, vol. 7, no. 1, p. 1441, 2017, doi: 10.1038/s41598-017-14844-5.

[27] J. Vappou, J. Luo, K. Okajima, M. Di Tullio, and E. E. Konofagou, "Non-invasive measurement of local pulse pressure by pulse wave-based ultrasound manometry (PWUM)," *Physiol. Meas.*, vol. 32, no. 10, pp. 1653–1662, Oct. 2011, doi: 10.1088/0967-3334/32/10/012.

[28] B. W. A. M. M. Beulen, N. Bijnens, G. G. Koutsouridis, P. J. Brands, M. C. M. Rutten, and F. N. van de Vosse, "Toward noninvasive blood pressure assessment in arteries by using ultrasound," *Ultrasound Med. Biol.*, vol. 37, no. 5, pp. 788–797, May 2011, doi: 10.1016/j.ultrasmedbio.2011.01.020.

[29] J. Seo, S. J. Pietrangelo, H. S. Lee, and C. G. Sodini, "Noninvasive arterial blood pressure waveform monitoring using two- Element ultrasound system," *IEEE Trans. Ultrason. Ferroelectr. Freq. Control*, vol. 62, no. 4, pp. 776–784, Apr. 2015, doi: 10.1109/TUFFC.2014.006904.

[30] A. Chandrasekhar, C.-S. S. Kim, M. Naji, K. Natarajan, J.-O. O. Hahn, and R. Mukkamala, "Smartphone-based blood pressure monitoring via the oscillometric finger-pressing method.," *Sci. Transl. Med.*, vol. 10, no. 431, Mar. 2018, doi: 10.1126/scitranslmed.aap8674.

[31] A. Chandrasekhar, K. Natarajan, M. Yavarimanesh, and R. Mukkamala, "An iPhone application for blood pressure monitoring via the oscillometric finger pressing method," *Sci. Rep.*, vol. 8, no. 13136, pp. 1–6, 2018, doi: 10.1038/s41598-018-31632-x.

[32] T. G. Papaioannou *et al.*, "Accuracy of commercial devices and methods for noninvasive estimation of aortic systolic blood pressure a systematic review and meta-analysis of invasive validation studies," *J. Hypertens.*, vol. 34, no. 7, pp. 1237–1248, 2016, doi: 10.1097/HJH.0000000000000921.

[33] C. M. McEniery, J. R. Cockcroft, M. J. Roman, S. S. Franklin, and I. B. Wilkinson, "Central blood pressure: Current evidence and clinical importance," *Eur. Heart J.*, vol. 35, no. 26, pp. 1719–1725, 2014, doi: 10.1093/eurheartj/eht565.

[34] G. Pucci *et al.*, "Evaluation of the Vicorder, a novel cuff-based device for the noninvasive estimation of central blood pressure," *J. Hypertens.*, vol. 31, no. 1, pp. 77–85, Jan. 2013, doi: 10.1097/HJH.0b013e32835a8eb1.

[35] T. Weber *et al.*, “Validation of a brachial cuff-based method for estimating central systolic blood pressure,” *Hypertension*, vol. 58, no. 5, pp. 825–832, 2011, Accessed: Jun. 25, 2017. [Online]. Available: http://hyper.ahajournals.org/content/58/5/825.long.

[36] W. J. Verberk, H.-M. Cheng, L.-C. Huang, C.-M. Lin, Y.-P. Teng, and C.-H. Chen, “Practical suitability of a stand-alone oscillometric central blood pressure monitor: A review of the Microlife WatchBP Office Central.,” *Pulse*, vol. 3, pp. 205–16, Apr. 2016, doi: 10.1159/000443771.

[37] D. Agnoletti, S. Millasseau, J. Topouchian, M. E. Safar, and J. Blacher, “Comparison of central blood pressure devices on the basis of a modified protocol of the European Society of Hypertension: application to the Centron cBP301,” *Blood Press. Monit.*, vol. 19, no. 2, pp. 103–108, Apr. 2014, doi: 10.1097/MBP.0000000000000028.

[38] X. Peng, M. G. Schultz, W. P. Abhayaratna, M. Stowasser, and J. E. Sharman, “Comparison of central blood pressure estimated by a cuff-based device with radial tonometry,” *Am. J. Hypertens.*, vol. 29, no. 10, pp. 1173–1178, Oct. 2016, doi: 10.1093/ajh/hpw063.

[39] F. Liang, “Numerical validation of a suprasystolic brachial cuff-based method for estimating aortic pressure,” *Biomed. Mater. Eng.*, vol. 24, no. 1, pp. 1053–1062, Jan. 2014, doi: 10.3233/BME-130903.

[40] I. G. Horváth *et al.*, “Invasive validation of a new oscillometric device (Arteriograph) for measuring augmentation index, central blood pressure and aortic pulse wave velocity,” *J. Hypertens.*, vol. 28, no. 28, pp. 2068–2075, 2019, doi: 10.1097/HJH.0b013e32833c8a1a.

[41] Y.-T. Shih, H.-M. Cheng, S.-H. Sung, W.-C. Hu, and C.-H. Chen, “Quantification of the calibration error in the transfer function-derived central aortic blood pressures,” *Am. J. Hypertens.*, vol. 24, no. 12, pp. 1312–1317, Dec. 2011, doi: 10.1038/ajh.2011.146.

[42] H.-M. Cheng, D. Lang, C. Tufanaru, and A. Pearson, “Measurement accuracy of non-invasively obtained central blood pressure by applanation tonometry: A systematic review and meta-analysis,” *Int. J. Cardiol.*, vol. 167, no. 5, pp. 1867–1876, 2013, doi: 10.1016/j.ijcard.2012.04.155.

[43] M. Gao, W. C. Rose, B. Fetics, D. A. Kass, C.-H. H. Chen, and R. Mukkamala, “A simple adaptive transfer function for deriving the central blood pressure waveform from a radial blood pressure waveform,” *Sci. Rep.*, vol. 6, no. 1, p. 33230, Sep. 2016, doi: 10.1038/srep33230.

[44] H.-M. Cheng *et al.*, “Estimation of central systolic blood pressure using an oscillometric blood pressure monitor,” *Hypertens. Res.*, vol. 33, no. 6, pp. 592–599, Jun. 2010, doi: 10.1038/hr.2010.37.

[45] Y.-T. Shih, H.-M. Cheng, S.-H. Sung, W.-C. Hu, and C.-H. Chen, “Comparison of two

generalized transfer functions for measuring central systolic blood pressure by an oscillometric blood pressure monitor," *J. Hum. Hypertens.*, vol. 27, no. 3, pp. 204–210, Mar. 2013, doi: 10.1038/jhh.2012.17.

[46] "American national standard for manual, electronic or automated sphygmomanometers," *Association for the Advancement of Medical Instrumentation.*, 2003. https://fmc4me.qa-intranet.fmcna.com/idc/idcplg?IdcService=GET_FILE&Rendition=Primary&RevisionSelectionMethod=Latest&dDocName=PDF_100032384 (accessed Aug. 30, 2018).

[47] G. W. Snedecor and W. G. Cochran, *Statistical methods*. Iowa State University Press, 1980.

[48] D. L. Newman, S. E. Greenwald, and N. L. Bowden, "An in vivo study of the total occlusion method for the analysis of forward and backward pressure waves.," *Cardiovasc. Res.*, vol. 13, no. 10, pp. 595–600, Oct. 1979, Accessed: Jun. 25, 2017. [Online]. Available: http://www.ncbi.nlm.nih.gov/pubmed/519662.

[49] H.-M. Cheng, S.-H. Sung, Y.-T. Shih, S.-Y. Chuang, W.-C. Yu, and C.-H. Chen, "Measurement accuracy of a stand-alone oscillometric central blood pressure monitor: A validation report for Microlife WatchBP Office Central," *Am. J. Hypertens.*, vol. 26, no. 1, pp. 42–50, Jan. 2013, doi: 10.1093/ajh/hps021.

[50] H.-M. Cheng, S.-H. Sung, Y.-T. Shih, S.-Y. Chuang, W.-C. Yu, and C.-H. Chen, "Measurement of central aortic pulse pressure: Noninvasive brachial cuff-based estimation by a transfer function vs. a novel pulse wave analysis method," *Am. J. Hypertens.*, vol. 25, no. 11, pp. 1162–1169, Nov. 2012, doi: 10.1038/ajh.2012.116.

[51] J. Lee *et al.*, "Physical basis of the relationship between central arterial blood pressure and distal pulse volume waveforms," *IEEE J. Biomed. Heal. Informatics*, 2017.

[52] J.-O. O. Hahn, A. T. Reisner, F. A. Jaffer, and H. H. Asada, "Subject-specific estimation of central aortic blood pressure using an individualized transfer function: A preliminary feasibility study," *IEEE Trans. Inf. Technol. Biomed.*, vol. 16, no. 2, pp. 212–220, Mar. 2012, doi: 10.1109/TITB.2011.2177668.

[53] D. Agnoletti *et al.*, "Pulse pressure amplification, pressure waveform calibration and clinical applications," *Atherosclerosis*, vol. 224, no. 1, pp. 108–112, Sep. 2012, doi: 10.1016/j.atherosclerosis.2012.06.055.

[54] S. Lewington, R. Clarke, N. Qizilbash, R. Peto, and R. Collins, "Age-specific relevance of usual blood pressure to vascular mortality: A meta-analysis of individual data for one million adults in 61 prospective studies," *Lancet*, vol. 360, no. 9349, pp. 1903–1913, Dec. 2002, doi: 10.1016/S0140-6736(02)11911-8.

[55] R. Mukkamala and J.-O. O. Hahn, "Toward ubiquitous blood pressure monitoring via pulse transit time: Predictions on maximum calibration period and acceptable error

limits," *IEEE Trans. Biomed. Eng.*, vol. 65, no. 6, pp. 1–11, Jun. 2018, doi: 10.1109/TBME.2017.2756018.

[56] J. Chamary, "Forbes : 3D Touch In iPhone 6S Isn't Just A Gimmick. Here's How It Works." https://www.forbes.com/sites/jvchamary/2015/09/12/3d-touch-iphone-6s/#30f4fdd44cee (accessed Sep. 06, 2018).

[57] "Apple Developer Documentation : UIKit." https://developer.apple.com/documentation/UIKit (accessed Sep. 06, 2018).

[58] J. C. Wu, "Statistical analysis of widths and heights of fingerprint images in terms of ages from segmentation data," 2008. Accessed: Aug. 24, 2018. [Online]. Available: https://www.nist.gov/sites/default/files/finger_size_age.pdf.

[59] "FMS Finapres Medical Systems | The Finapres NOVA has received 510(k) clearance from the US FDA!" http://www.finapres.com (accessed Jul. 17, 2020).

[60] D. Reisinger, "Fortune: Apple's iPhone X Sales Have Been Strong – But Not Record-Breaking, Analyst Says." http://fortune.com/2018/01/23/apple-iphone-x-sales-2/ (accessed Sep. 06, 2018).

[61] Mobilegeeks.de, "YouTube : Huawei Mate S Force Touch Demo [english]." https://www.youtube.com/watch?v=ta6beOvyhYE (accessed Sep. 06, 2018).

[62] "Statista: Share of iPhone installed base worldwide by model, as of April 2017." https://www.statista.com/statistics/755593/iphone-model-device-market-share-worldwide/ (accessed Sep. 06, 2018).

[63] "ISO 81060-2:2018 - Non-invasive sphygmomanometers -- Part 2: Clinical investigation of intermittent automated measurement type," 2018. https://www.iso.org/standard/73339.html (accessed Jul. 17, 2020).

[64] "Forbes: 2019 iPhone X To Have Virtual Fingerprint Reader, Smaller Notch: Report." https://www.forbes.com/sites/jeanbaptiste/2018/02/06/2019-iphone-x-to-have-virtual-fingerprint-reader-smaller-notch-report/#7cb44ee64f76 (accessed Sep. 06, 2018).

[65] "MotionEvent | Android Developers." https://developer.android.com/reference/android/view/MotionEvent (accessed Dec. 23, 2019).

[66] M. Lemay, M. Bertschi, J. Sola, P. Renevey, J. Parak, and I. Korhonen, "Chapter 2.3. Application of optical heart rate monitoring," in *Wearable Sensors: Fundamentals, Implementation and Applications*, E. Sazonov and M. R. Neuman, Eds. Academic Press, 2014, pp. 105–129.

[67] W. Flügge and W. Flügge, "Viscoelastic Models," in *Viscoelasticity*, Springer Berlin

Heidelberg, 1975, pp. 4–33.

[68] R. C. Block *et al.*, “Conventional pulse transit times as markers of blood pressure changes in humans,” *Sci. Rep.*, vol. 10, no. 1, pp. 1–9, 2020.

[69] J. C. Ruiz-Rodríguez *et al.*, “Innovative continuous non-invasive cuffless blood pressure monitoring based on photoplethysmography technology,” *Intensive Care Med.*, vol. 39, no. 9, pp. 1618–1625, 2013.

[70] M. Kachuee, M. M. Kiani, H. Mohammadzade, and M. Shabany, “Cuffless blood pressure estimation algorithms for continuous health-care monitoring,” *IEEE Trans. Biomed. Eng.*, vol. 64, no. 4, pp. 859–869, 2016.

[71] N. Watanabe *et al.*, “Development and validation of a novel cuff-less blood pressure monitoring device,” *JACC Basic to Transl. Sci.*, vol. 2, no. 6, pp. 631–642, Dec. 2017, doi: 10.1016/j.jacbts.2017.07.015.

[72] M. Radha *et al.*, “Estimating blood pressure trends and the nocturnal dip from photoplethysmography,” *Physiol. Meas.*, vol. 40, no. 2, p. 25006, 2019.

[73] X. Xing *et al.*, “Robust blood pressure estimation from finger photoplethysmography using age-dependent linear models,” *Physiol. Meas.*, vol. 41, no. 2, p. 025007, 2020.

[74] X. Xing, Z. Ma, M. Zhang, Y. Zhou, W. Dong, and M. Song, “An unobtrusive and calibration-free blood pressure estimation method using photoplethysmography and biometrics,” *Sci. Rep.*, vol. 9, no. 1, pp. 1–8, 2019.

[75] D. Nachman *et al.*, “Comparing blood pressure measurements between a photoplethysmography-based and a standard cuff-based manometry device,” *Sci. Rep.*, vol. 10, no. 1, pp. 1–9, 2020.

[76] E. A. Hines Jr and G. E. Brown, “The cold pressor test for measuring the reactibility of the blood pressure: Data concerning 571 normal and hypertensive subjects,” *Am. Heart J.*, vol. 11, no. 1, pp. 1–9, Jan. 1936, doi: 10.1016/S0002-8703(36)90370-8.

[77] J. Abrams, “Hemodynamic effects of nitroglycerin and long-acting nitrates,” *Am. Heart J.*, vol. 110, no. 1, pp. 217–224, 1985.

[78] M. Al’Absi, S. Bongard, T. Buchanan, G. A. Pincomb, J. Licinio, and W. R. Lovallo, “Cardiovascular and neuroendocrine adjustment to public speaking and mental arithmetic stressors,” *Psychophysiology*, vol. 34, no. 3, pp. 266–275, 1997.

[79] C. N. Joseph *et al.*, “Slow breathing improves arterial baroreflex sensitivity and decreases blood pressure in essential hypertension,” *Hypertension*, vol. 46, no. 4, pp. 714–718, 2005.

[80] M. Elgendi, “On the analysis of fingertip photoplethysmogram signals,” *Curr. Cardiol. Rev.*, vol. 8, no. 1, pp. 14–25, 2012.

[81] P. S. Addison, “Slope transit time (STT): A pulse transit time proxy requiring only a single signal fiducial point,” *IEEE Trans. Biomed. Eng.*, vol. 63, no. 11, pp. 2441–2444, 2016.

[82] J. M. Bland and D. G. Altman, “Agreement between methods of measurement with multiple observations per individual,” *J. Biopharm. Stat.*, vol. 17, no. 4, pp. 571–582, 2007.

[83] Efron B and Tibshirani RJ, “An introduction to the bootstrap,” *Chaprnan Hall. New York. EEUU*, 1993.

[84] S. Holm, “A simple sequentially rejective multiple test procedure,” *Scand. J. Stat.*, pp. 65–70, 1979.

[85] D. Fujita and A. Suzuki, “Evaluation of the possible use of PPG waveform features measured at low sampling rate,” *IEEE Access*, vol. 7, pp. 58361–58367, 2019.

[86] A. Chandrasekhar, M. Yavarimanesh, K. Natarajan, J.-O. Hahn, and R. Mukkamala, “PPG sensor contact pressure should be taken into account for cuff-less blood pressure measurement,” *IEEE Trans. Biomed. Eng.*, pp. 1–1, Feb. 2020, doi: 10.1109/tbme.2020.2976989.